Maternal age affects equine Day 8 embryo gene expression both in trophoblast and inner cell mass

E. Derisoud[1,2], L. Jouneau[1,2], C. Dubois[3], C. Archilla[1,2], Y. Jaszczyszyn[4], R. Legendre[5], N. Daniel[1,2], N. Peynot[1,2], M. Dahirel[1,2], J. Auclair-Ronzaud[3], L. Wimel[3], V. Duranthon[1,2], P. Chavatte-Palmer[1,2]*

[1] Université Paris-Saclay, UVSQ, INRAE, BREED, 78350, Jouy-en-Josas, France

[2] Ecole Nationale Vétérinaire d'Alfort, BREED, 94700, Maisons-Alfort, France

[3] IFCE, Plateau technique de la Valade, Chamberet, France

[4] Institute for Integrative Biology of the Cell (I2BC), UMR 9198 CNRS, CEA, Paris-Sud University F-91198, Gif-sur-Yvette, France

[5] Institut Pasteur—Bioinformatics and Biostatistics Hub—Department of Computational Biology, USR 3756 IP CNRS, Paris, France

*Corresponding author

Grant support:

This work was supported by the "Institut Français du Cheval et de l'Equitation" (grant number CS_2018_23, 2018). The National Research Institute for Agriculture, Food and Environment (INRAE) department Animal Physiology and Breeding Systems also supported this research.

Correspondence:

Emilie Derisoud

Domaine de Vilvert
Bâtiment 230-231, UMR 1198 BREED, INRAE
78350, Jouy-en-Josas, FRANCE

emilie.derisoud@gmail.com

Pascale Chavatte-Palmer

Domaine de Vilvert
Bâtiment 230-231, UMR 1198 BREED, INRAE
78350, Jouy-en-Josas, France

pascale.chavatte-palmer@inrae.fr

Abstract

Background: Breeding a mare until she is not fertile or even until her death is common in equine industry but the fertility decreases as the mare age increases. Embryo loss due to reduced embryo quality is partly accountable for this observation. Here, the effect of mare's age on blastocysts' gene expression was explored. Day 8 post-ovulation embryos were collected from multiparous young (YM, 6-year-old, N = 5) and older (OM, > 10-year-old, N = 6) non-nursing Saddlebred mares, inseminated with the semen of one stallion. Pure or inner cell mass (ICM) enriched trophoblast, obtained by embryo bisection, were RNA sequenced. Deconvolution algorithm was used to discriminate gene expression in the ICM from that in the trophoblast. Differential expression was analyzed with embryo sex and diameter as cofactors. Functional annotation and classification of differentially expressed genes and gene set enrichment analysis were also performed.

Results: Maternal aging did not affect embryo recovery rate, embryo diameter nor total RNA quantity. In both compartments, the expression of genes involved in mitochondria and protein metabolism were disturbed by maternal age, although more genes were affected in the ICM. Mitosis, signaling and adhesion pathways and embryo development were decreased in the ICM of embryos from old mares. In trophoblast, ion movement pathways were affected.

Conclusions: This is the first study showing that maternal age affects gene expression in the equine blastocyst, demonstrating significant effects as early as 10 years of age. These perturbations may affect further embryo development and contribute to decreased fertility due to aging.

Introduction

58 Unlike other farm animals, the main purpose for the use of horses is athletic performance and
59 leisure. In many cases, mares produce foals regularly to remain profitable after their sport career so
60 that their reproductive career may last until advanced age, even though mares' fertility declines with
61 age (for review [1]). Indeed, in Thoroughbreds, pregnancy rates per estrous at Day 42 post-ovulation
62 were shown to be reduced from 63.0% in young mares to 58.5% in mares older than 9 years of age,
63 and to reach 43.8% in mares older than 18 years old [2]. It is difficult to determine an age limit defining
64 when a mare is considered too old for breeding as aging is a progressive process during the life. One
65 study on 535,746 fertility records in mixed breeds in France, however, suggested that if a 10% of
66 fertility decline is chosen as cutoff value for retiring breeding mares, then mares older than 8 should
67 not be bred [3].
68 Embryo loss seems to be the principal cause for the fertility decline in old mares. Using pregnancy
69 data obtained from 898 cycles in Thoroughbred mares over period of 11 years, the cutoff for embryo
70 mortality to reach values above average was calculated to be 10 years of age [4]. In practice, embryo
71 loss frequency is generally observed between the first (14 - 22 days) and the second (42 - 45 days)
72 pregnancy check in old than in young mares [2,4,5]. Embryo loss may, however, be unobserved in earlier
73 stages. Indeed, although experimental oviductal flushes on Day 2 post-ovulation showed that the
74 fertilization rate was similar between young and fertile mares *vs* old and subfertile mares
75 (respectively, 10/14 *vs* 11/14 embryos recovered per group on Day 2), when the same mares were
76 inseminated during another estrus period, the pregnancy rate was significantly higher at 14 days post
77 ovulation in young and fertile mares compared to older ones (respectively, 12/15 *vs* 3/15 pregnant
78 mares on Day 14 by ultrasonography) [6].
79 Although uterine degeneration [7–9] is observed in old mares, oocyte quality seems to play a major role
80 in the observed age-related fertility decrease: the transfer of Day 4 embryos collected from old and
81 subfertile mares resulted in lower pregnancy rates at 14 days post-ovulation than when embryos
82 collected from young and fertile mares were transferred. This remained true when only the subset of
83 good quality embryos was considered [10].

84 Controversial effects of maternal age on oocyte morphology have been observed in several studies
85 [11–15] but there is a clear effect of maternal age on oocyte quality and function. Old mares' oocytes are
86 less likely to reach metaphase II after *in vitro* maturation than oocytes from younger mares [11].
87 Alterations of the expression of several genes have been also observed during *in vivo* and *in vitro*
88 oocyte maturation [16,17]. Moreover, after *in vitro* maturation, higher spindle instability is observed in
89 old versus young mares' oocytes, resulting in increased risks of chromosome misalignment leading to
90 embryo aneuploidy [18–20]. Controversial effects of mare age on mitochondria degeneration have been
91 also reported [16,21–23].
92 The effect of maternal age on embryo size is not so clear, as studies demonstrated a reduction of
93 embryo diameter in old mares at several developmental stages [24–28] while others did not detect any
94 effect [9,13,25,29] of maternal aging on embryo size. In these studies, however, the developmental stage
95 was not uniform and the method to measure embryo size could be different (direct measurement or
96 using ultrasonography). Furthermore, the size of the equine embryo is highly variable for the same
97 gestational age [30]. The only study that directly measured more than 200 Day 7 to 10 embryos as part
98 of an embryo transfer program observed that maternal aging induced a reduction in embryo size (in
99 average, more than 740µm in diameter for embryos produced by mares younger than 15 *vs* less than
100 620µm in diameter for embryos produced by mares older than 16) [31].
101 Maternal age, however, seems to affect embryo morphology from the earliest stages of
102 development. Embryos collected *in vivo* on Day 1.5 post ovulation, indeed, had the same number of
103 cells, but a poorer morphology grade (uniformity of cell size and texture, imperfections and
104 abnormalities) when they had been collected from mares older than 15 years of age compared to
105 young ones [32]. In addition, at Day 3 post ovulation, embryos collected from mares older than 20 years
106 of age combined poorer morphology grade and reduced cell number [32]. In contrast, in other studies,
107 no difference according to maternal age was observed in terms of number, size or texture of
108 blastomeres of embryos collected in oviducts on Days 2 and 4 post ovulation [6,10]. Finally, at blastocyst

109 stage, a higher incidence of morphological abnormalities was observed in embryos that were
110 collected from subfertile and/or 18 years old mares compared to 4 years old nulliparous mares [24].
111 Only a few studies have examined the effect of maternal age on equine embryo quality. As observed
112 in oocytes, metabolic function and capacity were reduced in Day 2 embryos collected from old mares
113 (≥20 years old) compared to those collected from young mares (≤14 years old) [22]. Moreover, a
114 reduced quantity of mitochondrial DNA, but not genomic DNA, has been reported in Day 7
115 blastocysts from mares older than 16 years of age compared to younger counterparts, suggesting a
116 reduction in mitochondria/cell ratio in old mares' blastocysts [23]. Taken together, these alterations
117 could lead to the alterations in embryo mobility and/or day of fixation that have been observed in
118 some studies [9,28].
119 Altogether, these data indicate that the quality of embryos is reduced in older mares. Considering
120 the Developmental Origins of Health and Diseases (DOHaD) [33], dam age could thus also affect feto-
121 placental and post-natal growth as well as long-term offspring health. To the authors' knowledge, the
122 effect of maternal age on gene expression in the equine embryo, however, has not yet been
123 explored.
124 The aim of this study was to determine the effect of maternal age in the mare on embryo gene
125 expression at the blastocyst stage. Young (<10 years) and older (>10 years) multiparous mares were
126 inseminated with the same stallion. Blastocysts were collected on Day 8 post-ovulation and bisected
127 to separate the pure trophoblast (TE_part) from the inner cell mass enriched hemi-embryo
128 (ICMandTE). Gene expression was analyzed by RNA-seq in each compartment. Deconvolution was
129 used to isolate gene expression of inner cell mass from trophoblast cells in ICMandTE part.

130

131 **Methods**

132 *Ethics*

133 The experiment was performed at the experimental farm of IFCE (research agreement C1903602
134 valid until March 22, 2023). The protocol was approved by the local animal care and use committee
135 ("Comité des Utilisateurs de la Station Expérimentale de Chamberet") and by the regional ethical
136 committee ("Comité Régional d'Ethique pour l'Expérimentation Animale du Limousin", approved
137 under N° C2EA - 33 in the National Registry of French Ethical Committees for animal
138 experimentation) under protocol number APAFIS#14963-2018050316037888 v2. All experiments
139 were performed in accordance with the European Union Directive 2010/63EU. The authors complied
140 with the ARRIVE guidelines.

141

142 *Embryo collection*

143 Thirty-one non-nursing multiparous Saddlebred mares (French Anglo-Arabian and Selle Français
144 breeds) were included in this study. Multiparous mares were defined as dams that had already foaled
145 at least once. Mares were bred and raised in the "Institut Français du Cheval et de l'Equitation"
146 experimental farm (Chamberet, France, 45° 34'55.17"N, 1°43'16.29"E, 442m). During the
147 experimental protocol, mares were managed in herds in natural pastures 24h/day with free access to
148 water. The experiments took place from April 1st to May 23rd, 2019. All mares remained healthy
149 during this period.

150 Mares were allocated to 2 groups according to their age: young mares (YM, < 10 years, n = 11) and
151 older mares (OM, ≥ 10 years, n = 20). The age threshold was defined in accordance with the
152 literature [3,4]. Before experimentation, mare's withers' height was measured. During the
153 experimentation, mares were weighted and mares' body condition score (BCS, scale 1 to 5) was
154 determined by one trained operator [88].

155 The mares' estrous period was monitored routinely by ultrasound with a 5MHz trans-rectal
156 transducer. During estrus, ovulation was induced with a single injection of human chorionic

157 gonadotropin (i.v.; 750 - 1500IU; Chorulon® 5000; MSD Santé animale, France) as soon as one
158 ovarian follicle > 35mm in diameter was observed, together with marked uterine edema. Ovulation
159 usually takes place within 48h, with > 80% occurring 25 to 48h after injection [89,90]. At the same time,
160 mares were inseminated once with fresh or fresh overnight cooled semen containing at least 1 billion
161 motile spermatozoa from a single fertile stallion. Ovulation was confirmed within the next 48 hours
162 by ultrasonography.

163 Embryos were collected by non-surgical uterine lavage using prewarmed (37°C) lactated Ringer's
164 solution (B.Braun, France) and EZ-Way Filter (IMV Technologies, France) 10 days after insemination,
165 i.e. approximately 8 days post ovulation. Just after embryo collection, mares were treated with
166 luprotiol an analogue of prostaglandin F2α (i.m; 7.5 mg; Prosolvin, Virbac, France).

167 The aim of the embryo collection was to obtain 5 embryos/group with each embryo coming from a
168 different mare. Therefore, some mares that failed to produce an embryo at their first attempt had
169 been bred again.

170

171 *Embryo bisection and RNA extraction*

172 Collected embryos were immediately observed using a binocular magnifier and photographed with a
173 size standard. Embryo diameter was subsequently determined on photographs using ImageJ®
174 software (version 1.52a; National Institutes of Health, Bethesda, MD, USA). Embryos were washed 4
175 times in commercially available Embryo holding medium (IMV Technologies, France) at 34°C and
176 then bisected with a microscalpel under binocular magnifying glass to separate trophoblast part, at
177 this stage composed of trophectoderm and endoderm (TE_part) from inner cell mass (composed of
178 epiblast cells) enriched hemi-embryos (ICMandTE) (Figure 1). Each hemi-embryo was transferred to
179 an Eppendorf DNA LoBind tube (Eppendorf, Montesson, France) with extraction buffer (PicoPure

180 RNA isolation kit, Applied Biosystems, France) and incubated for 30 min at 42°C prior to storage at -
181 80°C.

182 RNA was extracted from each hemi-embryo following the manufacturer's instructions using PicoPure
183 RNA isolation kit (PicoPure RNA isolation kit, Applied Biosystems, France), which included a DNAse
184 treatment. RNA quality and quantity were assessed with the 2100 Bioanalyzer system using RNA
185 6000 Pico or nano kit (Agilent Technologies, France) according to the manufacturer's instructions
186 (Supplementary Figure S1).

187

188 *RNA sequencing*

189 Five nanograms of total RNA were mixed (Supplementary Figure S1) with ERCC spike-in mix
190 (Thermofisher Scientific, France) according to manufacturer recommendations. Messenger RNAs
191 were reverse transcribed and amplified using the SMART-Seq V4 ultra low input RNA kit (Clontech,
192 France) according to the manufacturer recommendations. Nine PCR cycles were performed for each
193 hemi-embryo. cDNA quality was assessed on an Agilent Bioanalyzer 2100, using an Agilent High
194 Sensitivity DNA Kit (Agilent Technologies, France). Libraries were prepared from 0.15 ng cDNA using
195 the Nextera XT Illumina library preparation kit (Illumina, France). Libraries were pooled in equimolar
196 proportions and sequenced (Paired end 50-34 pb) on NextSeq500 instrument, using a NextSeq 500
197 High Output 75 cycles kit (Illumina, France) (Supplementary Figure S1). Demultiplexing was
198 performed with bcl2fastq2 version 2.2.18.12 (Illumina, France) and adapters were trimmed with
199 Cutadapt version 1.15 [91]. Only reads longer than 10pb were kept.

200

201 *Embryo sexing*

202 Embryo sex was determined for each embryo in order to take in consideration embryo sex in the
203 statistical analysis as sexual dimorphism was observed in blastocysts in other species [92].

204 The expression of *X Inactive Specific Transcript* (*XIST*) was analyzed. *XIST* is a long noncoding RNA
205 from chromosome X responsible for X inactivation when two X chromosomes are present, meaning
206 that only female embryos express *XIST*. *XIST* was shown to be expressed in equine female blastocysts
207 on Day 8 post ovulation [35,38]. *XIST* is not annotated in the available equine Ensembl 3.0.99 or NCBI
208 annotation. Thus, a *de novo* transcript assembly was made using StringTie version 2.1.2 [93] following
209 manufacturer instructions to identify *XIST* in equine embryo samples (Supplementary Figure S1). The
210 genome annotation file output was aligned on Ensembl 99 EquCab3.0 assembly using IGV version
211 2.7.2 [94]. As *XIST* position and length on X chromosome has been previously determined [35] and as *XIST*
212 is annotated in humans, the most similar contig was selected. The obtained *XIST* sequence was
213 22,600 bp long and composed of 8 exons and 7 introns. *XIST* sequence was added to FASTA files from
214 Ensembl 99 EquCab3.0 assembly and to the genome annotation file from Ensembl 99 EquCab3.0
215 assembly as a unique fictitious chromosome with one gene composed of one transcript.

216 *XIST* expression differed between individuals but was relatively close in quantification between
217 related hemi-embryos. Therefore, seven embryos were determined as females (4 in the YM group
218 and 3 in the OM group) while 4 were considered as males (1 in the YM group, and 3 in the OM
219 group).

220

221 *RNA mapping and counting*

222 Alignment was performed using STAR version 2.6 [95] (2-pass mapping with the genome annotation file
223 using the following parameters: --alignSoftClipAtReferenceEnds No --alignEndsType EndToEnd --
224 alignIntronMax 86545 --alignMatesGapMax 86545) on previously modified Ensembl 99 EquCab3.0
225 assembly and annotation. Genes were then counted with featureCounts [96] from Subreads package
226 version 1.6.1 (parameters: -p -B -C -M) (Supplementary Figure S1).

227

228 *Data analysis*

229 All statistical analyses were performed by comparing OM to YM (set as reference group) using R
230 version 4.0.2 [97] on Rstudio software version 1.3.1056 [98].

231

232 ***Embryo recovery rate, embryo diameter and total RNA content analysis***

233 Embryo recovery rate (ERR) per mare was calculated as number of attempts with at least one
234 embryo collected/total number of attempts. ERR per ovulation was determined as number of
235 collected embryos/total number of observed ovulations. They were analyzed using the Exact Fisher
236 test to determine if age influences ERR.

237 For total RNA content analysis, as embryos were bisected without strict equality for each hemi-
238 embryo, a separate analysis of ICMandTE and TE_part RNA quantities would not be meaningful. Thus,
239 ICMandTE and TE_part RNA quantities were initially summed up and analyzed using a mixed linear
240 model from nlme package version 3.1-148 [99], followed by 1000 permutations using PermTest
241 function from pgirmess package version 1.6.9 [100]. Maternal age and embryo sex were considered as
242 random effects.

243 Embryo diameter was analyzed with a fixed effects linear model of nlme package version 3.1-148 [99]
244 including maternal age and embryo sex, followed by 1000 permutations using PermTest function
245 from pgirmess package version 1.6.9 [100]. Variables were kept in models when statistically significant
246 differences were observed. Differences were considered as significant for $p < 0.05$.

247 Moreover, the relation between embryo size and total RNA quantity/embryo was studied and
248 represented using the nonlinear regression analysis (fitness to exponential growth equation) in
249 GraphPad Prism software 8.0.1 for Windows (Graphpad Software, San Diego, California USA,
250 www.graphpad.com).

251

252 ***Deconvolution of gene expression in ICMandTE using DeMixT***

253 A filter on counts obtained with featureCounts was applied: all genes with more than 3 non null
254 count values in at least one group (OM or YM) per hemi-embryo (ICMandTE or TE_part) were
255 conserved. The ICMandTE hemi-embryo was composed of both trophoblast and inner cell mass in
256 unknown relative proportions. In order to estimate the relative gene expression of both cell types,
257 the DeMixT R package version 1.4.0 was used [101,102]. Starting from a dataset obtained from one cell
258 type, DeMixT estimates the proportion of cells in the mixed samples and performs a deconvolution
259 algorithm on gene expression. TE_part (reference cells) and ICMandTE (mixed cells type) datasets
260 were thus analyzed using the following options: niter=10; nbin=50; if.filter=TRUE;
261 ngene.selected.for.pi=1500; ngene. Profile.selected=1500; nspikein=0. Since the deconvolution
262 algorithm cannot be performed in the presence of null values, the value "1" was added to all count
263 values in ICMandTE and TE_part data tables. Moreover, variance in reference cell dataset (TE_part)
264 must not be null and gene with null variance had been removed prior to the deconvolution. Output
265 datasets were DeMixT_ICM_cells and DeMixT_TE_cells, corresponding to the deconvoluted gene
266 expression in ICM cells and TE cells of ICMandTE, respectively.

267

268 ***Quality checks for deconvolution***

269 At the end of deconvolution, a quality check is automatically performed by the analysis: for every
270 gene, if the difference of average of deconvoluted expression of reference cells in mixed samples
271 (here, gene expression of TE cells in ICMandTE dataset, *i.e.,* DeMixT_TE_cells) and average of
272 expression of reference cells (here, gene expression of TE cells in TE_part) is > 4, then, the
273 deconvolution for concerned genes is not reliable. Therefore, genes in this case are filtered out.

274 Moreover, outputs of DeMixT_ICM_cells *vs* DeMixT_TE_cells, DeMixT_ICM_cells *vs* TE_part and
275 ICMandTE *vs* TE_part were compared with Deseq2 version 1.28.1 [103] to confirm that the
276 deconvolution was effective at separating gene expression. Moreover, several genes proper to ICM

277 and TE cells in equine embryos were identified using literature search [35]. Their raw and deconvoluted
278 expressions were analyzed to check the reliability of deconvolution. Results of these analyses were
279 represented through manually drawn Venn diagrams as well as principal component analysis (PCA)
280 graphics of individuals, using FactoMineR version 2.4 [104], ggplot2 version 3.3.3 [105] and factoextra
281 version 1.0.7 [106].

282

283 ***Maternal age comparison for gene expression***

284 For the comparison of maternal age, ICMandTE, DeMixT_ICM_cells and TE_part datasets were used
285 and a filter was applied on datasets: all genes with an average expression equal or above 10 counts in
286 at least one group (OM or YM) per hemi-embryo (ICM or TE) were conserved. Differential analyses
287 were performed with Deseq2 version 1.28.1 [103] with YM group as reference, without independent
288 filtering. Genes were considered differentially expressed (DEG) for FDR < 0.05 after Benjamini-
289 Hochberg correction (also known as false discovery rate, FDR). As ovulation was checked only every
290 48h and because embryos growth is exponential in the uterus, embryo diameter was considered as a
291 cofactor in the model as well as embryo sex. Moreover, PCAs using factominer version 2.4 [104]on R
292 software followed with a Partial redundancy analysis using rda function from vegan package version
293 2.5-7 [107] were performed. For these analyses, embryo size was considered as a factor of two
294 modalities: embryos < 1100µm were considered as small and > 1100µm were considered as large.
295 Results were represented with a biplot graphic using the package factoextra version 1.0.7 [106]. The
296 combined analyses were used to represent and determine the specific contribution of each of the
297 two factors in the total variability observed in DEGs. The objective was to verify that the age of the
298 mare was the main factor explaining the difference between the DEGs and not the differences in
299 embryo size. On biplot graphics, only the 20 variables, *i.e.,* genes, that contributed the most in axis
300 construction, were represented.

301 Equine Ensembl IDs were converted into Human Ensembl IDs and Entrez Gene names using gorth
302 function in gprofiler2 package version 0.1.9 [108]. Genes without Entrez Gene names using gprofiler2
303 were manually converted when Entrez Gene names were available, using Ensembl web search
304 function [109].

305 Moreover, DEG were analyzed for classification, over- and under- representation (FDR < 0.05) using
306 Fisher's exact test corrected with FDR and using the database Gene Ontology (GO) Biological Process
307 complete on PANTHER version 16.0 web-based software [110]. Only the most specific subclass
308 pathways, provided by PANTHER's automated hierarchy sorting, were conserved and represented.

309

310 ***Gene set enrichment analyses (GSEA)***

311 The count values were log transformed using RLOG function of DESeq2 version 1.28.1. Gene set
312 enrichment analyses (GSEA) were performed on expressed genes using GSEA software version 4.0.3
313 (Broad Institute, Inc., Massachusetts Institute of Technology, and Regents of the University of
314 California) [111,112] to identify biological gene sets disturbed by age. GSEA was performed using the
315 following parameters: 1000 gene set permutations, weighted enrichment analysis, gene set size
316 between 15 and 500, signal-to-noise metrics. Molecular Signatures Database [113] version 7.1 (C2:
317 KEGG: Kyoto Encyclopedia of Genes and Genomes, C5: BP: GO biological process) were used to
318 identify most perturbed pathways. Pathways were considered significantly enriched for FDR < 0.05.
319 When normalized enrichment score (NES) was positive, the gene set was enriched in the OM group
320 while when NES was negative, the gene set was enriched in the YM group.

321 Enriched terms from GO BP and KEGG database were represented using SUMER analysis from
322 SUMER R package version 1.1.5 and using FDR q-values [114]. First, SUMER analysis reduces redundancy
323 using weighted set cover algorithm and then clusters the results using affinity propagation algorithm.
324 The weighted set cover algorithm performs a selection of the fewest number of gene sets that
325 include all genes associated with the enriched sets, giving priority for the most significant terms.

326 Then, the affinity propagation algorithm groups similar gene sets and identifies one representative
327 gene set. This algorithm will repeat this clustering to obtain the most representative gene sets.
328 Results were represented with graph modified using Cytoscape version 3.8.2 [115]. Gene sets were
329 represented by nodes and the gene set size was represented by the size of the node. Node shape
330 represented the gene set database (GO BP or KEGG). Blue nodes represented gene sets enriched in
331 YM (NES < 0) while red nodes represented gene sets enriched in OM (NES > 0). Edge width represents
332 the level of connection between representative gene sets (thinner edges represent the first
333 clustering while thicker edges represent the second clustering of the affinity propagation algorithm)

334

335 Data availability statement

336 The datasets generated during and/or analyzed during the current study are available in the GEO
337 repository,

338 [accession: GSE162893; https://www.ncbi.nlm.nih.gov/geo/query/acc.cgi?acc=GSE162893].

339

340 Results

341 Altogether, 36 uterine flushings were performed (12 in YM <10 years old and 24 in OM >10 years old)
342 to obtain one embryo per mare. For 5 mares, after a negative embryo collection, a second attempt
343 was performed. Characteristics of mares are detailed in Table 1. One YM and 3 OM had a double
344 ovulation but no twin embryo was obtained. Embryo recovery rates (ERR) per mare and per
345 ovulation were, respectively, 42% and 39% in YM and 25% and 22% in OM, with no significant
346 difference between groups ($p = 0.45$ for ERR/mare and $p = 0.46$ for ERR/ovulation). All embryos were
347 expanded blastocysts, grade I or II according to the embryo classification of McKinnon and Squires [34].

348 Embryo diameter ranged from 409 µm to 2643 µm, with no effect of group on embryo diameter (p =
349 0.97). RNA yield per embryo ranged from 16 ng to 2915.5 ng and was not related to mares' age (p =
350 0.92). There is a clear exponential relation between RNA yield/embryo and embryo size (Figure 2a).
351 The median RNA Integrity Number (RIN) was 9.8 (8.7 - 10 range). Between 29.4 and 69.5 million
352 reads per sample were obtained after trimming. On average, 83.61% of reads were mapped on the
353 modified EquCab 3.0 using STAR and 66.66% of reads were assigned to genes by featureCounts.
354
355 After keeping genes with less than 3 non null count values in at least one group (OM or YM) per
356 hemi-embryo (ICMandTE or TE_part), 16,741 genes were conserved for deconvolution. In addition,
357 twenty-seven genes were removed because their variance was null in the TE_part. However, for
358 these genes, the mean counting in ICMandTE samples was above 10 counts, excepted for one which
359 had a mean expression of 34 counts. On the other hand, this gene was only expressed in 5 ICMandTE
360 over the 10 counts threshold.
361 During the analysis, 3 additional genes were excluded because the deconvolution quality for these
362 genes was not sufficient. Therefore, at the end of deconvolution algorithm, 16,711 genes were
363 available for differential analysis.
364 Before deconvolution, 341 genes were differentially expressed (FDR < 0.05) between the ICMandTE
365 and the TE_part (Figure 3a). After deconvolution, comparison between DeMixT_ICM_cells and
366 DeMixT_TE_cells yielded 7,565 differentially expressed genes while the comparison
367 DeMixT_ICM_cells *vs* TE_part yielded 6,085 differentially expressed genes, with 5,925 in common
368 (72%). Moreover, except one of the initially 341 differentially expressed genes before deconvolution,
369 were also identified as differentially expressed in both post-deconvolution analyses. On the PCA
370 graphic of individuals, ICMandTE and TE_part were not really separated before deconvolution (Figure
371 3b). DeMixT_TE_cells and TE_part were partly superposed, suggesting that datasets before and after
372 deconvolution have a similar global gene expression; whereas the DeMixT_ICM_cells group is clearly

373 separated from both on Axis 2 (14.3% of variance), indicating that the deconvolution effectively
374 enabled the separation of gene expression in the two cell types.
375 Six of the 12 genes previously identified as more expressed in ICM [35] were also more expressed in
376 ICMandTE *vs* TE_part comparison (Table 2). After deconvolution (comparison DeMixT_ICM_cells *vs*
377 TE_part), 3 more genes previously identified were also differentially expressed. However, for two of
378 them (POU Class 5 Homeobox 1, *POU5F1* and Undifferentiated Embryonic Cell Transcription Factor 1,
379 *UTF1*), their expression was increased in TE_part after deconvolution. In TE, any genes previously
380 identified were differentially expressed in the comparison ICMandTE *vs* TE_part, *i.e.*, before
381 deconvolution. After deconvolution, the expression of 2 genes was increased in TE_part compared to
382 DeMixT_ICM_cells.
383 For further analysis, DeMixT_ICM_cells and TE_part gene expression datasets are presented.
384 Nevertheless, the comparison of maternal age on ICMandTE dataset (graphics, differential gene
385 expression analysis and GSEA) was also performed and this analysis is available in Supplementary
386 Figure S2 and supplementary Tables S1 and S2.
387
388 After filtering out of genes with an average expression < 10 counts/maternal age group/hemi-
389 embryo, 13,735 genes were considered as expressed in the ICM cells from OM or YM embryos
390 including 255 differentially expressed genes (227 downregulated and 28 upregulated in OM) (Figure
391 4a and Supplementary Table S3). Only 218 and 12 genes out of the down- and upregulated genes,
392 respectively, were associated to a known protein in human. These downregulated genes in ICM of
393 embryos from OM mainly belonged to cellular process, metabolic process and biological regulation in
394 GO biological process gene sets (Figure 4a). From downregulated genes in OM ICM, 84 pathways
395 were statistically overrepresented in GO Biological process leading to 16 most specific subclass
396 pathways according to hierarchy sorting by PANTHER (Figure 4b). Overrepresented pathways in
397 downregulated genes in OM ICM were linked to cell division, embryo morphogenesis, histone
398 methylation, protein modification processes and cytoskeleton organization.

399 Upregulated differentially expressed genes (DEG) in OM ICM were mainly part of biological
400 regulation, response to stimulus, cellular process, signaling and metabolic process in GO biological
401 process gene sets (Figure 4a). No pathway was statistically overrepresented in upregulated genes in
402 ICM of embryos from old mares using PANTHER overrepresentation testing.
403
404 In the TE, 13,178 genes were considered as expressed in OM or YM. Fourteen were differentially
405 expressed (Supplementary Table S4) with 11 genes being downregulated and 3 being up regulated in
406 OM (Figure 4a). Only 12 genes were associated to a known protein in human. Downregulated genes
407 in OM mainly belonged to both cellular and metabolic process in GO biological process gene sets.
408
409 As the embryo size was highly variable within each group, a PCA analysis was made on DEG in ICM
410 and TE to verify that observed differences were effectively due to maternal age more than to embryo
411 size (Figure 2b). Respectively 3 YM and 3 OM were classified in small (<1100µm in diameter) while
412 the remaining 2 YM and 3 OM were classified in large group (> 1100µm in diameter).
413 In the ICM, the first axis of the PCA explained 58.3% of the variance of the data and clearly separated
414 OM from YM, indicating than more than half of the variance in DEG is due to maternal aging. The
415 second axis slightly separated genes according to embryo size but explained only 11.9% of the
416 variance, indicating that in the ICM, embryo size explains a minor part of the variance. These
417 observations were confirmed by the Partial redundancy analysis. Indeed, in ICM, 43% of the variance
418 was explained by maternal age while only 14% was explained by embryo size. Moreover, the 20
419 variables that contributed the most to the separation are mostly explaining differences related to
420 maternal age.
421 In the TE part, both the first and the second axis (explaining respectively, 67.3% and 16.5% of data
422 variability) separated both maternal age and embryo size groups. The partial redundancy analysis
423 also showed a less clear impact of maternal age in DEG from TE. Indeed, mares' age explained 31% of
424 the variance of DEGs whereas 22% was explained by embryo size. Moreover, although most of genes

425 showed a clear contribution in the construction of the first axis, some such as cystathionine beta-
426 synthase (*CBS*) and CD69 molecule (*CD69*) were clearly involved in the construction of the second
427 axis.
428
429 After Entrez Gene ID conversion, 12,344 genes were considered expressed in ICM. In the GO
430 Biological Process database, 106 identified gene sets differed according to maternal age in the ICM
431 (11 enriched in OM and 95 enriched in YM) (Supplementary Table S5). In the KEGG database, 14 gene
432 sets were perturbed (Supplementary Table S5).
433 Using SUMER analysis (Figure 5), gene sets enriched in OM ICM were mainly grouped under terms
434 "Respiratory electron transport chain" and "Translational elongation". The first term represents
435 mitochondrial function while the second represents translation function. Moreover, terms relative to
436 "Systemic lupus erythematosus" are conserved by SUMER analysis and enriched in OM ICM. Genes
437 involved in these enrichments were also present in dysregulated metabolic pathways.
438 Gene sets enriched in YM ICM were involved in different biological processes such as "Mitotic
439 nuclear division" which is relative to mitosis. Under this term, "Spindle organization" and "Negative
440 regulation of supramolecular fiber organization" terms represent the assembly of spindle during
441 mitosis. "Chromosome segregation" is also found in this grouping. Furthermore, terms under "Golgi
442 vesicle transport" seem to be involved in cytokinesis and vesicle trafficking. The catabolism of protein
443 and mRNA is represented by "Ubiquitin mediated proteolysis". Translation function is represented by
444 several terms grouped under "covalent chromatin modification" in the mitosis part.
445 "Leukocyte transendothelial migration" term is also enriched in YM ICM and seems to represent cell
446 signaling and adhesion. Indeed, this term regroups several pathways such as "Focal adhesion",
447 "Adherens junction" and "WNT signaling pathway".
448 Finally, further terms related to embryo development could be found in different groups such as
449 "Dendrite development", "Cell differentiation in spinal cord" or "endothelial cell development".

450 After Entrez Gene ID conversion, 11,874 genes were considered expressed in TE from OM or YM
451 embryos. In GO BP database, 38 gene sets were perturbed by mares' age in the TE of embryos (11
452 enriched in YM and 27 enriched in OM) (Supplementary Table S6). In the KEGG database, 5 pathways
453 were enriched in the TE of OM embryos (Supplementary Table S6).
454 As in ICM part, using SUMER analysis, translation (represented by both "Translational termination"
455 and "Ribosome" terms) and mitochondrial function (represented by "Oxidative phosphorylation"
456 associated terms) were enriched in OM embryos. "Proteasome" term is enriched in OM embryos
457 representing protein catabolism.
458 Moreover, transcription (represented by "Peptidyl lysine trimethylation" term) and embryo
459 development (represented by "spinal cord development") were, as in ICM, also, enriched in YM
460 embryos. Finally, in TE, "Regulation of action potential" term and associated terms were enriched in
461 YM. These terms could be related to ion movement.
462

463 ## Discussion

464 Maternal aging did not affect embryo recovery rate (ERR), embryo size nor total RNA quantity. It is
465 important to notice that, as the experimental protocol required only 5 embryos per group, a limited
466 number of embryo collection attempts were performed, resulting in a limited statistical power for
467 these analyses. ERR, especially in young mares, was not as good as in commercial embryo transfer
468 programs [31,36]. Moreover, total RNA content in equine embryo was exponentially correlated to
469 embryo diameter and was not affected by maternal age.
470 As ovulation check was only performed 48 hours after induction of ovulation, there is a bias in the
471 estimation of the embryo age in the present study. This certainly partly explains the large variation in
472 embryo size observed here. Different studies, however, have shown that embryo size is highly
473 variable [37–39], even when ovulation determination is accurate to the nearest 6 hours [40]. Accurately
474 determining fertilization time *in vivo* is not possible and the size of 142 equine embryos recovered at

475 8 days post-ovulation was reported to range from 120 to 3,980µm with an average of 1,132µm [30]. In
476 the present project, all embryos remain within these limits.
477 Although embryo size could be considered as normal for Day 8 embryos, embryo sizes were highly
478 variable and not equally distributed between groups. Embryo size was considered as a cofactor in the
479 differential analysis. In addition, partial redundancy analysis showed that embryo size explained less
480 than 25% of the variability of DEGs in both ICM and TE. As effects of maternal age on equine embryo
481 growth are not so clear [24–28], an interaction between both effects on embryo gene expression can not
482 be excluded. Maternal age, however, explained 43 and 31% of the total variability of DEGs in both
483 ICM and TE, respectively, suggesting that identified DEGs were mainly due to maternal age effects. It
484 is important to note that in ICM, the proportion of variability explained by maternal age was 3 times
485 greater than that of embryo size, whereas in the TE, this difference was smaller. This could be
486 explained by the fewer number of DEGs identified in TE compared to ICM but also because
487 trophoblast expansion was possibly more correlated to embryo size than the ICM.
488 As in tumors, today, the only way to analyze separate expression of ICM and TE cells in mammalian
489 embryos is to use micromanipulation but micromanipulation is expensive in time and requires
490 adapted skills and material. In this study, micromanipulation to properly separate ICM and TE was
491 not possible. Therefore, deconvolution appeared to be a good option to analyze the effects of
492 maternal ICM gene expression in mixed ICM and TE samples. Deconvolution seemed to have been
493 effective on embryo to separate ICM and TE gene expression. Indeed, the 341 genes differentially
494 expressed in ICMandTE *vs* TE_part were also identified by comparing TE with post-deconvolution ICM
495 cells gene expression dataset. Moreover, after deconvolution, more genes were differentially
496 expressed between TE and ICM datasets and among them, more genes identified in literature were
497 differentially expressed. Finally, PCA showed that deconvolution separate DeMixT_ICM_cells from
498 other datasets while before deconvolution ICMandTE and TE_part were partly superposed. Only
499 POU5F1 and UTF1 differed in terms of allocation between previously published data [35] and the
500 present study. In data before deconvolution, expression of POU5F1 and UTF1 were extremely

501 variable according to embryo diameter in both compartments. Deconvolution reduced the variability
502 of both gene expression in ICM but not in TE. Studies showed that POU5F1 is expressed in both
503 compartments until Day 10 post ovulation in equine in vivo produced embryos [41] but its expression
504 decreases progressively from Day 7 in TE cells. Thus, the statistically increased expression of POU5F1
505 in TE on Day 8 is compatible with previously published data.
506 Therefore, it was chosen to only present the analysis of the effects of age in DeMixT_ICM_cells
507 dataset. In all cases, deconvolution did not change the principal results of maternal aging on embryo
508 gene expression because the comparison of maternal age in ICMandTE and DeMixT_ICM_cells gave
509 comparable results.
510 In both ICM and TE, the expression of genes involved in mitochondrial function and translation with
511 ribosome biogenesis were enriched in OM embryos while transcription with chromatin modification
512 was enriched in YM embryos (Figure 6). Mitosis, signaling and adhesion pathways were additionally
513 altered and the expression of genes involved in embryo development was particularly reduced in the
514 ICM hemi-embryos from old mares. Finally, in the TE, ion movement related genes were affected.
515 Several studies on mature oocytes in women and mice, using microarrays and RNAseq, had shown a
516 differential expression of genes involved in mitochondrial, cell cycle, cytoskeleton functions and
517 related pathways according to maternal age [42–44], as observed in the present study in equine
518 blastocysts, especially in the ICM. In equine follicles and oocytes, the expression of genes essential
519 for oocyte maturation, as studied by RT-qPCR, quantitatively and temporally differed with maternal
520 age, suggesting a desynchronization [16]. Moreover, a study on the expression of 48 genes that have
521 been previously identified as related to aneuploidy and maternal aging in humans showed
522 differential expression in cumulus-oocytes complexes from young (< 12 years of age) and old (> 18
523 years old) mares [17]. Genes related to mitochondrial replication and function were also down-
524 regulated in oocytes of old mares [23]. Even effects of maternal aging on gene expression in equine
525 oocytes, using high throughput techniques, are not yet available, results on equine Day 8 blastocysts
526 suggest that mitochondrial perturbations present in the oocyte persist until the blastocyst stage. In

527 humans, single-embryo RNA-seq analysis showed that maternal aging alters the transcriptome of
528 blastocysts derived from ICSI. Genes altered by maternal age were related to segregation of
529 chromosomes, embryonic growth and cell signaling [45,46], as observed in our study on equine
530 blastocysts.

531 Unlike the human embryo, the equine embryo remains spherical, grows very fast and is surrounded
532 by its glycoprotein capsule up to 22 days post ovulation [37]. At 8 days post ovulation, equine embryos
533 are therefore growing and the endodermal layer entirely delineates the future yolk sac (Figure 6) [47].
534 Moreover, whereas in Day 7 embryos, the epiblast is lined by a continuous layer of trophoblast
535 named the polar trophoblast. As the blastocyst grows, epiblast cells phagocyte polar trophoblast cells
536 that become discontinuous. During this time, epiblast and polar trophoblast cells divided and are
537 bound by tight junctions [48]. The turnover in focal adhesion is essential for cell movement and
538 phagocytosis [49].

539 Cell signaling and adhesion function were altered in OM embryos. Indeed, KEGG pathways "focal
540 adhesion" and "adherens junction" regrouped in “Leukocyte transendothelial migration” on Figure 4
541 are disturbed in old mares' embryos. Focal adhesions are subcellular structures observed in adherent
542 cells, that are clusters of different structural and signaling molecules and integrins that form a
543 physical link between the actin cytoskeleton and the extracellular matrix [50,51]. Integrins are the major
544 receptors for cell adherence to extracellular matrix proteins in focal adhesions by playing an
545 important role in transmembrane connections to the cytoskeleton and activation of several signaling
546 pathways, as growth factor receptors [52]. Integrin Subunit Alpha V (*ITGAV*) expression was reduced in
547 the ICM of embryos collected from OM. In different human breast cancer cell lines, cell proliferation,
548 invasion and renewal are restricted when *ITGAV* is inhibited [53].

549 Moreover, the activity and localization of small GTPases within the Rho family must be precisely
550 regulated as the communication between them is indispensable to achieve the turnover of actin
551 filaments and cell adhesions necessary for cell migration, that are essential processes for the proper
552 development of the embryo [54]. The Rho GTPase Activating Protein 9 and 35 (*ARHGAP9* and

553 *ARHGAP35*) were downregulated in OM ICM. *ARHGAP35* codes for P190 Rho GTPase activating
554 protein that mediates signalization through integrin-dependent adhesion in cells. Aberrant neural
555 morphogenesis, related to an accumulation of polymerized actin in embryoneural tube cells, is
556 reported in mice lacking P190 Rho GTPase activating proteins [55]. Furthermore, P21 activated kinases
557 (PAK) are effector kinases for other small Rho GTPases such as Rac that regulate the polymerization
558 of actin and can affect the microtubule organization [56]. Once activated, PAKs promote the turnover
559 of focal adhesions by regulating transcription [57]. *PAK3* was downregulated in the OM ICM. However,
560 in TE, SLIT-ROBO Rho GTPase Activating Protein 3, *SRGAP3* was one of the upregulated genes in OM.
561 This gene regulates cytoskeletal reorganization and plays an important role in the formation of cell-
562 cell adhesion [58]. Therefore, maternal aging seems to alter focal adhesion in both ICM and TE of
563 embryos but, while in ICM, it seems to reduce cohesion and signalization, in TE it seems to reinforce
564 them.
565 Several signaling pathways required for development were altered and numerous genes related to
566 focal adhesions and signaling pathways were down-regulated in OM ICM (*ARHGAP9* and *ARHGAP35*;
567 B-Raf Proto-Oncogene, Serine/Threonine Kinase, *BRAF*; Filamin C, *FLNC*; FYN Proto-Oncogene, Src
568 Family Tyrosine Kinase, *FYN*; *PAK3*; Protein Phosphatase 1 Regulatory Subunit 12A, *PPP1R12A*; Talin
569 2, *TLN2*; X-Linked Inhibitor Of Apoptosis, *XIAP*). Among all signaling pathways, transforming growth
570 factor beta (TGF-β), Wg et Int (Wnt), mitogen-activated protein kinases (MAPK) and apoptosis
571 signaling were altered by maternal age in equine embryos. Indeed, transforming growth factor beta
572 receptor 1 (*TGFBR1*) was downregulated in the ICM of embryos from old mares. *TGFBR1* is one of the
573 two dimers for the receptor for transforming growth factors beta that is essential in the generation
574 of axes and cell fate commitment during mammal embryogenesis [59]. Moreover, Casein Kinase 1
575 Alpha 1, (*CSNK1A1*) and *Protein* Phosphatase 2 Regulatory Subunit B'Epsilon (*PPP2R5E*), involved in
576 Wnt signaling pathway, were downregulated in OM embryos. Wnt signaling pathway is also involved
577 in nervous development system and may act on cell determination in mice embryos [60]. Moreover,

578 Doublesex And Mab-3 Related Transcription Factor 3 (*DMRT3*) was downregulated in the OM ICM.
579 *DMRT3* is required for the proper development of the brain in prenatal chicken and mice [61].
580 Cell cycle related pathways and genes were also disturbed by maternal aging. Indeed, the expression
581 of Pleckstrin Homology domain-Interacting Protein (*PHIP*), also known as replication initiation
582 determinant, was reduced in the OM ICM. This gene is required for the initiation of DNA replication.
583 Fibroblasts originated from mice embryos with depleted *PHIP* expression presented less replication-
584 initiation as well as abnormal replication fork progression events [62]. Moreover, several cyclins (CCN)
585 were less expressed in the ICM of embryos from old mares (*CCNB3*, *CCNI* and *CCNT2*). Cyclins are key
586 cell cycle regulators and, for instance cyclin B3 degradation allows the passage from metaphase
587 (chromatids aligned on metaphase plate) to anaphase (segregation of sister chromatids) [63]. During
588 metaphase and anaphase, spindle assembly and chromosome segregation could also be
589 compromised. Indeed, genes involved in the formation of microtubules (Tubulin Gamma 2, *TUBG2*)
590 [64], the generation of the mitotic spindle (Never in Mitosis A related kinase 9, *NEK9*) [65], the production
591 of cohesion and condensing complexes (Structural Maintenance Of Chromosomes 4, *SMC4*) [66], the
592 control of centriole length, important for centrosomes and microtubules organization (Centriolar
593 Coiled-Coil Protein 110, *CCP110*) [67], the amplification of intra-spindle microtubules allowing the
594 formation of a sufficient quantity of kinetochore (HAUS Augmin Like Complex Subunit 6, *HAUS6*) [68],
595 the stabilization and protection of the cohesin complex association with chromatin (Cell Division
596 Cycle Associated 5, *CDCA5*; Shugosin 2, *SGO2*) [69,70] and the production of microtubule-based motor
597 proteins (Kinesin Family Member 14 and 23, *KIF14* and *KIF23*) [71] were downregulated in OM ICM.
598 Furthermore, Centromere protein F (*CENPF*), an important regulator of chromosome segregation
599 during mitosis, was reduced in OM ICM. CENPF is indispensable for murine embryo development
600 from the first stages of development until at least the blastocyst stage [72]. Impaired *CENPF* expression
601 could induce chromosome mis-segregation in the ICM of old mares' embryos.
602 Cytokinesis seems to also be altered by maternal age. CD2-associated protein (*CD2AP*) and Vacuolar
603 Protein Sorting 4 Homolog A (*VPS4A*) were downregulated in OM ICM. Both are involved in the late

604 phase of cytokinesis which correspond to the abscission of the cell, producing two daughter cells [73,74].
605 Globally, results suggest that cell division is impaired or indicate that there is less division in the ICM
606 of old mares' embryos.
607 Transcription is regulated by epigenetic marks. Several pathways linked to methylation and
608 acetylation were enriched in YM ICM and TE in relation to numerous upregulated genes in YM ICM
609 (i.e., Histone Deacetylase 1 and 2, *HDAC1* and *HDAC2*; Helicase, Lymphoid Specific, *HELLS*; DNA
610 Methyltransferase 3 Alpha, *DNMT3A*; Lysine Acetyltransferase 6B, *KAT6B*; Lysine Demethylase 4A,
611 *KDM4A*; Lysine Methyltransferase 2A, *KMT2A*; Nuclear Receptor Binding SET Domain Protein 3,
612 *NSD3*; SET Domain Containing 5, *SETD5*; Tet Methylcytosine Dioxygenase 1, *TET1*). At blastocyst
613 stage, *de novo* methylation is more important in the inner cell mass than in trophoblast cells and is
614 essential for the proper development of mammalian embryos [75]. *DNMT3A* is essential for *de novo*
615 methylation and required for embryo viability [76]. As it has been shown that maternal aging increases
616 the acetylation of lysine 12 of histone H4 in mice oocytes, affecting fertilization and embryo
617 development [77], it is likely that the methylation and acetylation dysregulation observed in the
618 embryos of old mares could be inherited from the oocyte rather than directly due to embryo
619 environment.
620 Both in OM ICM and TE, several pathways related to mitochondrial function were enriched.
621 Mitochondria are long known to be the "powerhouse" of cells, producing most of the necessary ATP
622 for cellular function [78]. ATP production is possible through oxidative phosphorylation enabled by the
623 electron transport chain in the inner membrane of mitochondria. This process begins with the
624 oxidation of NADH or FADH that generates a proton gradient across the mitochondrial membrane,
625 driving ATP synthesis through the phosphorylation of ADP *via* ATPase [79]. Enriched pathways in OM
626 embryos demonstrate that the NADH dehydrogenase (complex I), the oxidoreductase acting on a
627 heme group of donors (complex III) with the global electron carrier, and the proton-transporting ATP
628 synthase (1^{rst} part of the complex V) activities were particularly enriched while the second part of
629 complex V is depleted. Since all complexes are required to produce ATP, the impaired complex

630 generation may lead to mitochondrial stress and uncoupled respiratory chain, resulting in poor ATP
631 production. In human IVF embryos, reduced mitochondrial respiration efficiency, with a negative
632 effect on embryo development, is observed when oocytes are collected from old women [80]. In
633 mammalian expanded blastocysts, energy requirement is high, probably because of the need for ion
634 transport enabling quick blastocoel cavity expansion. Defects in metabolic requirements during
635 blastocyst development are associated with impaired implantation [81]. Equine embryos are not an
636 exception [82].
637 Mitochondria being maternally inherited, uncoupling of the mitochondrial respiratory chain may
638 originate from mitochondrial defects already present in oocytes [83]. Studies have shown that, in
639 human, poor oocyte quality is responsible for the decline in fertility associated with maternal aging.
640 The reduced oocyte developmental competence in older women is related to mitochondrial
641 dysfunction [84]. In horses' oocytes, before *in vitro* maturation, no difference between young and old
642 mares is observed while after, reduced mitochondrial DNA copy numbers, increased swelling and
643 reduced mitochondrial cristae are reported in oocytes collected from mares >12 years. This suggests
644 that oocyte mitochondria from old mares present deficiencies that become problematic when energy
645 needs are high, as during *in vitro* maturation or subsequent embryo development [21]. Because
646 mitochondrial replication in equine embryos does not begin until the blastocyst stage [85], oocyte
647 mitochondrial numerical or functional deficiencies may compromise early embryogenesis.
648 In TE, the GO biological process "Regulation of action potential" and "Transmission nerve impulse",
649 related to ion movement, were enriched in YM embryos. These processes are associated with genes
650 involved in the action potential dependent ion channels. These ion channels such as NA^+, K^+, ATPase
651 are essential for the accumulation of blastocoel and subsequently yolk sac fluid in equine embryos [86].
652 Their inhibition is detrimental for embryo development [87]. Thus, both reduced ATP production and
653 disturbed ion channels' function may impact embryo growth, although effects of mares' age on
654 embryo growth are controversial [24–28].

655 This is the first study showing an effect of maternal age on gene expression in the equine blastocyst
656 at Day 8 post ovulation. Maternal age, even for mares as young as 10 years old, disturbs several
657 processes related to chromatin segregation, cytokinesis, apposition of epigenetic marks and
658 mitochondrial function and that the ICM appears to be more affected than the TE. These
659 perturbations on Day 8 post ovulation may affect the further development of the embryo and as a
660 result, may contribute to decreased fertility due to aging. So far, maternal age does not appear to
661 have an impact on foal morphology at birth but, as for placental function, more subtle effects may
662 exist. Here, as embryos were collected long before implantation, it is impossible to know if these
663 embryos would have implanted and if they would have produced a live foal or not. Studies on long-
664 term growth and health of foals born to the same mares are currently being performed.
665
666

667 ## References

668 1. Scoggin, C. F. Not just a number: effect of age on fertility, pregnancy and offspring vigour in
669 thoroughbred brood-mares. *Reprod. Fertil. Dev.* **27**, 872 (2015).
670 2. Allen, W. R., Brown, L., Wright, M. & Wilsher, S. Reproductive efficiency of Flatrace and
671 National Hunt Thoroughbred mares and stallions in England. *Equine Veterinary Journal* **39**, 438–
672 445 (2007).
673 3. Langlois, B. & Blouin, C. Statistical analysis of some factors affecting the number of horse births
674 in France. *Reprod. Nutr. Dev.* **44**, 583–595 (2004).
675 4. Malheiros de Souza, J. R. *et al.* Age-dependent effect of foal heat breeding on pregnancy and
676 embryo mortality rates in Thoroughbred mares. *Journal of Equine Veterinary Science* 102982
677 (2020) doi:10.1016/j.jevs.2020.102982.
678 5. Chevalier-Clément, F. Pregnancy loss in the mare. *Animal Reproduction Science* **20**, 231–244
679 (1989).
680 6. Ball, B. A., Little, T. V., Hillman, R. B. & Woods, G. L. Pregnancy rates at Days 2 and 14 and
681 estimated embryonic loss rates prior to day 14 in normal and subfertile mares. *Theriogenology*
682 **26**, 611–619 (1986).
683 7. Doig, P. A., McKNIGHT, J. D. & Miller, R. B. The Use of Endometrial Biopsy in the Infertile Mare.
684 *Can Vet J* **22**, 72–76 (1981).
685 8. Siemieniuch, M. J., Gajos, K., Kozdrowski, R. & Nowak, M. Advanced age in mares affects
686 endometrial secretion of arachidonic acid metabolites during equine subclinical endometritis.
687 *Theriogenology* **103**, 191–196 (2017).
688 9. Carnevale, E. M. & Ginther, O. J. Relationships of age to uterine function and reproductive
689 efficiency in mares. *Theriogenology* **37**, 1101–1115 (1992).
690 10. Ball, B. A., Little, T. V., Weber, J. A. & Woods, G. L. Survival of Day-4 embryos from young,
691 normal mares and aged, subfertile mares after transfer to normal recipient mares.
692 *Reproduction* **85**, 187–194 (1989).

693 11. Brinsko, S. P., Ball, B. A. & Ellington, J. E. In vitro maturation of equine oocytes obtained from
694 different age groups of sexually mature mares. *Theriogenology* **44**, 461–469 (1995).
695 12. Carnevale, E. *et al.* Comparison of oocytes from young and old mares with light and electron
696 microscopy. *Theriogenology* **51**, 299 (1999).
697 13. Frank, B. L., Doddman, C. D., Stokes, J. E. & Carnevale, E. M. Association of equine oocyte and
698 cleavage stage embryo morphology with maternal age and pregnancy after intracytoplasmic
699 sperm injection. *Reprod. Fertil. Dev.* **31**, 1812 (2019).
700 14. Carnevale, E. M., Coutinho da Silva, M. A., Panzani, D., Stokes, J. E. & Squires, E. L. Factors
701 affecting the success of oocyte transfer in a clinical program for subfertile mares.
702 *Theriogenology* **64**, 519–527 (2005).
703 15. Altermatt, J. L., Suh, T. K., Stokes, J. E. & Carnevale, E. M. Effects of age and equine follicle-
704 stimulating hormone (eFSH) on collection and viability of equine oocytes assessed by
705 morphology and developmental competency after intracytoplasmic sperm injection (ICSI).
706 *Reprod. Fertil. Dev.* **21**, 615 (2009).
707 16. Campos-Chillon, F., Farmerie, T. A., Bouma, G. J., Clay, C. M. & Carnevale, E. M. Effects of aging
708 on gene expression and mitochondrial DNA in the equine oocyte and follicle cells. *Reprod.*
709 *Fertil. Dev.* **27**, 925 (2015).
710 17. Cox, L., Vanderwall, D. K., Parkinson, K. C., Sweat, A. & Isom, S. C. Expression profiles of select
711 genes in cumulus–oocyte complexes from young and aged mares. *Reprod. Fertil. Dev.* **27**, 914
712 (2015).
713 18. Rizzo, M. *et al.* Compromised MPS1 Activity Induces Multipolar Spindle Formation in Oocytes
714 From Aged Mares: Establishing the Horse as a Natural Animal Model to Study Age-Induced
715 Oocyte Meiotic Spindle Instability. *Front. Cell Dev. Biol.* **9**, 657366 (2021).
716 19. Rizzo, M. *et al.* The horse as a natural model to study reproductive aging-induced aneuploidy
717 and weakened centromeric cohesion in oocytes. *aging* (2020) doi:10.18632/aging.104159.

718 20. Rizzo, M. *et al.* Advanced mare age impairs the ability of in vitro-matured oocytes to correctly
719 align chromosomes on the metaphase plate. *Equine Vet J* **51**, 252–257 (2019).
720 21. Rambags, B. P. B. *et al.* Advancing maternal age predisposes to mitochondrial damage and loss
721 during maturation of equine oocytes in vitro. *Theriogenology* **81**, 959–965 (2014).
722 22. Catandi, G. D. *et al.* Equine maternal aging affects oocyte lipid content, metabolic function and
723 developmental potential. *Reproduction* **161**, 399–409 (2021).
724 23. Hendriks, W. K. *et al.* Maternal age and in vitro culture affect mitochondrial number and
725 function in equine oocytes and embryos. *Reprod. Fertil. Dev.* **27**, 957 (2015).
726 24. Woods, G. L., Baker, C. B., Hillman, R. B. & Schlafer, D. H. Recent studies relating to early
727 embryonic death in the mare. *Equine Veterinary Journal* **17**, 104–107 (1985).
728 25. Carnevale, E. M., Griffin, P. G. & Ginther, O. J. Age-associated subfertility before entry of
729 embryos into the uterus in mares. *Equine Veterinary Journal* **25**, 31–35 (1993).
730 26. Brinsko, S. P., Ball, B. A., Miller, P. G., Thomas, P. G. A. & Ellington, J. E. In vitro development of
731 day 2 embryos obtained from young, fertile mares and aged, subfertile mares. *Reproduction*
732 **102**, 371–378 (1994).
733 27. Willmann, C., Schuler, G., Hoffmann, B., Parvizi, N. & Aurich, C. Effects of age and altrenogest
734 treatment on conceptus development and secretion of LH, progesterone and eCG in early-
735 pregnant mares. *Theriogenology* **75**, 421–428 (2011).
736 28. Camargo Ferreira, J. *et al.* Luteal vascularity and embryo dynamics in mares during early
737 gestation: Effect of age and endometrial degeneration. *Reprod Dom Anim* **54**, 571–579 (2019).
738 29. Morel, M. C. G. D., Newcombe, J. R. & Swindlehurst, J. C. The effect of age on multiple ovulation
739 rates, multiple pregnancy rates and embryonic vesicle diameter in the mare. *Theriogenology*
740 **63**, 2482–2493 (2005).
741 30. Vanderwall, D. K. Early Embryonic Development and Evaluation of Equine Embryo Viability.
742 *Veterinary Clinics of North America: Equine Practice* **12**, 61–83 (1996).

743 31. Panzani, D., Rota, A., Marmorini, P., Vannozzi, I. & Camillo, F. Retrospective study of factors
744 affecting multiple ovulations, embryo recovery, quality, and diameter in a commercial equine
745 embryo transfer program. *Theriogenology* **82**, 807–814 (2014).
746 32. Carnevale, E. M., Bergfelt, D. R. & Ginther, O. J. Aging effects on follicular activity and
747 concentrations of FSH, LH, and progesterone in mares. *Animal Reproduction Science* **31**, 287–
748 299 (1993).
749 33. Chavatte-Palmer, P., Velazquez, M. A., Jammes, H. & Duranthon, V. Review: Epigenetics,
750 developmental programming and nutrition in herbivores. *Animal* **12**, s363–s371 (2018).
751 34. McKinnon, A. O. & Squires, E. L. Morphologic assessment of the equine embryo. *Journal of the*
752 *American Veterinary Medical Association* **192**, 401–406 (1988).
753 35. Iqbal, K., Chitwood, J. L., Meyers-Brown, G. A., Roser, J. F. & Ross, P. J. RNA-Seq Transcriptome
754 Profiling of Equine Inner Cell Mass and Trophectoderm. *Biology of Reproduction* **90**, (2014).
755 36. Marinone, A. I. *et al.* The effect of mare's age on multiple ovulation rate, embryo recovery,
756 post-transfer pregnancy rate, and interovulatory interval in a commercial embryo transfer
757 program in Argentina. *Animal Reproduction Science* **158**, 53–59 (2015).
758 37. Betteridge, K. J., Eaglesome, M. D., MITCHELLt, D., Flood, P. F. & Beriault, R. Development of
759 horse embryos up to twenty two days after ovulation: observations on fresh specimens. *Journal*
760 *of Anatomy* **135**, 191–209 (1982).
761 38. Beckelmann, J., Budik, S., Bartel, C. & Aurich, C. Evaluation of Xist expression in preattachment
762 equine embryos. *Theriogenology* **78**, 1429–1436 (2012).
763 39. Colchen, S. *et al.* Quantitative histological analysis of equine embryos at exactly 156 and 168 h
764 after ovulation. *J Reprod Fertil Suppl* 527–537 (2000).
765 40. Leisinger, C. A., Medina, V., Markle, M. L., Paccamonti, D. L. & Pinto, C. R. F. Morphological
766 evaluation of Day 8 embryos developed during induced aluteal cycles in the mare.
767 *Theriogenology* **105**, 178–183 (2018).

768 41. Hisey, E., Ross, P. J. & Meyers, S. A. A Review of OCT4 Functions and Applications to Equine
769 Embryos. *Journal of Equine Veterinary Science* **98**, 103364 (2021).
770 42. Grøndahl, M. L. *et al.* Gene expression profiles of single human mature oocytes in relation to
771 age. *Human Reproduction* **25**, 957–968 (2010).
772 43. Reyes, J. M. *et al.* Differing molecular response of young and advanced maternal age human
773 oocytes to IVM. *Human Reproduction* **32**, 2199–2208 (2017).
774 44. Hamatani, T. *et al.* Age-associated alteration of gene expression patterns in mouse oocytes.
775 *Human Molecular Genetics* **13**, 2263–2278 (2004).
776 45. Kawai, K. *et al.* Parental age and gene expression profiles in individual human blastocysts. *Sci*
777 *Rep* **8**, 2380 (2018).
778 46. McCallie, B. R. *et al.* Compromised global embryonic transcriptome associated with advanced
779 maternal age. *J Assist Reprod Genet* **36**, 915–924 (2019).
780 47. Enders, A. C., Schlafke, S., Lantz, K. C. & Liu, I. K. M. Endoderm cells of the equine yolk sac from
781 Day 7 until formation of the definitive yolk sac placenta. *Equine Veterinary Journal* **25**, 3–9
782 (1993).
783 48. Enders, A. C., Lantz, K. C., Liu, I. K. M. & Schlafke, S. Loss of polar trophoblast during
784 differentiation of the blastocyst of the horse. *Journal of Reproduction and Fertility* **83**, 447–460
785 (1988).
786 49. Hauck, C. R., Hsia, D. A. & Schlaepfer, D. D. The Focal Adhesion Kinase--A Regulator of Cell
787 Migration and Invasion. *IUBMB life* **53**, 115–119 (2002).
788 50. Provenzano, P. P. & Keely, P. J. Mechanical signaling through the cytoskeleton regulates cell
789 proliferation by coordinated focal adhesion and Rho GTPase signaling. *Journal of Cell Science*
790 **124**, 1195–1205 (2011).
791 51. Zhao, X. & Guan, J.-L. Focal adhesion kinase and its signaling pathways in cell migration and
792 angiogenesis. *Advanced Drug Delivery Reviews* **63**, 610–615 (2011).
793 52. Hynes, R. O. Integrins: bidirectional, allosteric signaling machines. *Cells* **110**, 673–687 (2002).

794 53. Cheuk, I. W.-Y., Siu, M. T., Ho, J. C.-W., Chen, J. & Shin, V. Y. ITGAV targeting as a therapeutic
795 approach for treatment of metastatic breast cancer. *American Journal of Cancer Research* **10**,
796 211–223 (2020).
797 54. Riento, K. & Ridley, A. J. ROCKs: multifunctional kinases in cell behaviour. *Nat Rev Mol Cell Biol*
798 **4**, 446–456 (2003).
799 55. Brouns, M. R. p190 RhoGAP is required for neural development. *Development* **127**, 4891–4903
800 (2000).
801 56. Rane, C. K. & Minden, A. P21 activated kinases: Structure, regulation, and functions. *Small*
802 *GTPases* **5**, e28003 (2014).
803 57. Chan, P. M., Lim, L. & Manser, E. PAK Is Regulated by PI3K, PIX, CDC42, and PP2Cα and
804 Mediates Focal Adhesion Turnover in the Hyperosmotic Stress-induced p38 Pathway. *J. Biol.*
805 *Chem.* **283**, 24949–24961 (2008).
806 58. Bacon, C., Endris, V. & Rappold, G. A. The cellular function of srGAP3 and its role in neuronal
807 morphogenesis. *Mechanisms of Development* **130**, 391–395 (2013).
808 59. Wu, M. Y. & Hill, C. S. TGF-β Superfamily Signaling in Embryonic Development and Homeostasis.
809 *Developmental Cell* **16**, 329–343 (2009).
810 60. Kemp, C., Willems, E., Abdo, S., Lambiv, L. & Leyns, L. Expression of all Wnt genes and their
811 secreted antagonists during mouse blastocyst and postimplantation development. *Dev. Dyn.*
812 **233**, 1064–1075 (2005).
813 61. Smith, C. A., Hurley, T. M., McClive, P. J. & Sinclair, A. H. Restricted expression of DMRT3 in
814 chicken and mouse embryos. *Mechanisms of Development* **119**, S73–S76 (2002).
815 62. Zhang, Y. *et al.* A replicator-specific binding protein essential for site-specific initiation of DNA
816 replication in mammalian cells. *Nat Commun* **7**, 11748 (2016).
817 63. Yuan, K. & O'Farrell, P. H. Cyclin B3 Is a Mitotic Cyclin that Promotes the Metaphase-Anaphase
818 Transition. *Current Biology* **25**, 811–816 (2015).

819 64. Vinopal, S. *et al.* γ-Tubulin 2 Nucleates Microtubules and Is Downregulated in Mouse Early
820 Embryogenesis. *PLoS ONE* **7**, e29919 (2012).
821 65. Fry, A. M., O'Regan, L., Sabir, S. R. & Bayliss, R. Cell cycle regulation by the NEK family of protein
822 kinases. *Journal of Cell Science* **125**, 4423–4433 (2012).
823 66. Losada, A. & Hirano, T. Shaping the metaphase chromosome: coordination of cohesion and
824 condensation. *Bioessays* **23**, 924–935 (2001).
825 67. Schmidt, T. I. *et al.* Control of Centriole Length by CPAP and CP110. *Current Biology* **19**, 1005–
826 1011 (2009).
827 68. Watanabe, S., Shioi, G., Furuta, Y. & Goshima, G. Intra-spindle Microtubule Assembly Regulates
828 Clustering of Microtubule-Organizing Centers during Early Mouse Development. *Cell Reports*
829 **15**, 54–60 (2016).
830 69. Ladurner, R. *et al.* Sororin actively maintains sister chromatid cohesion. *EMBO J* **35**, 635–653
831 (2016).
832 70. Rivera, T. & Losada, A. Shugoshin and PP2A, shared duties at the centromere. *Bioessays* **28**,
833 775–779 (2006).
834 71. Welburn, J. P. I. The molecular basis for kinesin functional specificity during mitosis.
835 *Cytoskeleton* **70**, 476–493 (2013).
836 72. Zhou, C.-J. *et al.* Loss of CENPF leads to developmental failure in mouse embryos. *Cell Cycle* **18**,
837 2784–2799 (2019).
838 73. Monzo, P. *et al.* Clues to CD2-associated Protein Involvement in Cytokinesis□D □V. *Molecular*
839 *Biology of the Cell* **16**, 12 (2005).
840 74. Babst, M. & Davies, B. A. Regulation of Vps4 During MVB Sorting and Cytokinesis. *Traffic* **12**,
841 1298–1305 (2011).
842 75. Hales, B. F., Grenier, L., Lalancette, C. & Robaire, B. Epigenetic programming: From gametes to
843 blastocyst. *Birth Defects Research Part A: Clinical and Molecular Teratology* **91**, 652–665 (2011).

844 76. Marcho, C., Cui, W. & Mager, J. Epigenetic dynamics during preimplantation development.
845 *REPRODUCTION* **150**, R109–R120 (2015).
846 77. Suo, L. *et al.* Changes in acetylation on lysine 12 of histone H4 (acH4K12) of murine oocytes
847 during maternal aging may affect fertilization and subsequent embryo development. *Fertility*
848 *and Sterility* **93**, 945–951 (2010).
849 78. Dumollard, R., Duchen, M. & Carroll, J. The Role of Mitochondrial Function in the Oocyte and
850 Embryo. in *The mitochondrion in the germline and early development* vol. 77 21–49 (Elsevier,
851 2007).
852 79. Balaban, R. S., Nemoto, S. & Finkel, T. Mitochondria, Oxidants, and Aging. *Cell* **120**, 483–495
853 (2005).
854 80. Wilding, M. *et al.* Mitochondrial aggregation patterns and activity in human oocytes and
855 preimplantation embryos. *Human Reproduction* **16**, 909–917 (2001).
856 81. Gardner, D. K. & Harvey, A. J. Blastocyst metabolism. *Reprod. Fertil. Dev.* **27**, 638 (2015).
857 82. Lane, M., O'Donovan, M. K., Squires, E. L., Seidel, G. E. & Gardner, D. K. Assessment of
858 metabolism of equine morulae and blastocysts. *Mol. Reprod. Dev.* **59**, 33–37 (2001).
859 83. Hutchison, C. A., Newbold, J. E., Potter, S. S. & Edgell, M. H. Maternal inheritance of mammalian
860 mitochondrial DNA. *Nature* **251**, 536–538 (1974).
861 84. Krisher, R. L. Maternal age affects oocyte developmental potential at both ends of the age
862 spectrum. *Reprod. Fertil. Dev.* **31**, 1 (2019).
863 85. Hendriks, W. K. *et al.* Mitochondrial DNA replication is initiated at blastocyst formation in
864 equine embryos. *Reprod. Fertil. Dev.* **31**, 570 (2019).
865 86. Waelchli, R. O., MacPhee, D. J., Kidder, G. M. & Betteridge, K. J. Evidence for the Presence of
866 Sodium- and Potassium-Dependent Adenosine Triphosphatase alpha 1 and beta 1 Subunit
867 Isoforms and Their Probable Role in Blastocyst Expansion in the Preattachment Horse
868 Conceptus. *Biology of Reproduction* **57**, 630–640 (1997).

869 87. Nascimento, A. D. do *et al.* Inhibition of Na+, K+ -ATPase with ouabain is detrimental to equine
870 blastocysts. *Anim Reprod* **17**, e20190079 (2020).
871 88. Arnaud, M. G., Dubroeucq, M. H. & Rivot, M. D. *Notation de l'état corporel des chevaux de selle*
872 *et de sport: guide pratique*. (Institut de l'élevage, 1997).
873 89. Duchamp, G., Bour, B., Combarnous, Y. & Palmer, E. Alternative solutions to hCG induction of
874 ovulation in the mare. *J Reprod Fertil Suppl* **35**, 221–228 (1987).
875 90. Bucca, S. & Carli, A. Efficacy of human chorionic gonadotropin to induce ovulation in the mare,
876 when associated with a single dose of dexamethasone administered at breeding time: Efficacy
877 of human chorionic gonadotropin to induce ovulation when associated with dexamethasone.
878 *Equine Veterinary Journal* **43**, 32–34 (2011).
879 91. Martin, M. Cutadapt removes adapter sequences from high-throughput sequencing reads.
880 *EMBnet. journal* **17**, 10–12 (2011).
881 92. Gutiérrez-Adán, A. *et al.* Developmental Consequences of Sexual Dimorphism During Pre-
882 implantation Embryonic Development. *Reprod Domest Anim* **41**, 54–62 (2006).
883 93. Pertea, M. *et al.* StringTie enables improved reconstruction of a transcriptome from RNA-seq
884 reads. *Nat Biotechnol* **33**, 290–295 (2015).
885 94. Robinson, J. T. *et al.* Integrative genomics viewer. *Nat Biotechnol* **29**, 24–26 (2011).
886 95. Dobin, A. *et al.* STAR: ultrafast universal RNA-seq aligner. *Bioinformatics* **29**, 15–21 (2013).
887 96. Liao, Y., Smyth, G. K. & Shi, W. featureCounts: an efficient general purpose program for
888 assigning sequence reads to genomic features. *Bioinformatics* **30**, 923–930 (2014).
889 97. R Core Team. *A Language and Environment for Statistical Computing*. https://www.R-
890 project.org/ (2020).
891 98. Rstudio Team. *RStudio: Integrated Development for R. RStudio*. (PBC, 2020).
892 99. Pinheiro, J., Bates, D., Debroy, S., Sarkar, D. & R Core Team. *nlme: Linear and Nonlinear Mixed*
893 *Effects Models*. (2020).
894 100. Giraudoux, P. *pgirmess: Spatial Analysis and Data Mining for Field Ecologists*. (2018).

895 101. Cao, S. *et al.* Differing total mRNA expression shapes the molecular and clinical phenotype of
896 cancer. *bioRxiv* 57 (2020) doi:10.1101/2020.09.30.306795.
897 102. Wang, Z. *et al.* Transcriptome Deconvolution of Heterogeneous Tumor Samples with Immune
898 Infiltration. *iScience* **9**, 451–460 (2018).
899 103. Love, M. I., Huber, W. & Anders, S. Moderated estimation of fold change and dispersion for
900 RNA-seq data with DESeq2. *Genome Biol* **15**, 550 (2014).
901 104. Lê, S., Josse, J. & Husson, F. FactoMineR: An R Package for Multivariate Analysis. *J. Stat. Soft.* **25**,
902 1:18 (2008).
903 105. Gómez-Rubio, V. **ggplot2** - Elegant Graphics for Data Analysis (2nd Edition). *J. Stat. Soft.* **77**,
904 (2017).
905 106. Kassambara, A. & Mundt, F. *factoextra: Extract and Visualize the Results of Multivariate Data*
906 *Analyses*. (2020).
907 107. Oksanen, J. *et al. vegan: Community Ecology Package*. (2020).
908 108. Kolberg, L. & Raudvere, U. *gprofiler2: Interface to the 'g:Profiler' Toolset.* (2020).
909 109. Yates, A. D. *et al.* Ensembl 2020.
910 110. Mi, H. *et al.* PANTHER version 16: a revised family classification, tree-based classification tool,
911 enhancer regions and extensive API. *Nucleic Acids Research* **49**, D394–D403 (2021).
912 111. Subramanian, A. *et al.* Gene set enrichment analysis: A knowledge-based approach for
913 interpreting genome-wide expression profiles. *Proceedings of the National Academy of Sciences*
914 **102**, 15545–15550 (2005).
915 112. Mootha, V. K. *et al.* PGC-1α-responsive genes involved in oxidative phosphorylation are
916 coordinately downregulated in human diabetes. *Nat Genet* **34**, 267–273 (2003).
917 113. Liberzon, A. *et al.* The Molecular Signatures Database Hallmark Gene Set Collection. *Cell*
918 *Systems* **1**, 417–425 (2015).
919 114. Savage, S. R., Shi, Z., Liao, Y. & Zhang, B. Graph Algorithms for Condensing and Consolidating
920 Gene Set Analysis Results. *Molecular & Cellular Proteomics* **18**, S141–S152 (2019).

921 115. Shannon, P. Cytoscape: A Software Environment for Integrated Models of Biomolecular
922 Interaction Networks. *Genome Research* **13**, 2498–2504 (2003).
923

Acknowledgments

The authors are grateful to the staff of the Institut Français du Cheval et de l'Equitation (IFCE) experimental farm (Domaine de la Valade, Chamberet, France) for care and management of animals. We acknowledge the High-throughput sequencing facility of I2BC for its sequencing and bioinformatics expertise. The bioinformatics analyses were performed thanks to Core Cluster of the Institut Français de Bioinformatique (IFB) (ANR-11-INBS-0013). Many thanks to Matthias Zytnicki and Christophe Klopp for their advice on RNA-seq de novo analysis. Many thanks to Pablo Ross who kindly provided the coordinates for the XIST gene. The authors thank Denis Laloe for its help with vegan package. The authors thank Shavahn Loux for her information on PLAC8A. The authors are grateful to Alice Jouneau, Sophie Calderari and Patrice Humblot who kindly revised this article.

Author contributions

PCP obtained the funding. PCP and VD conceived the project. LW, PCP, and VD supervised the study. ED, CD, CA, ND, NP, LW, VD and PCP adapted the methodology for the project. ED, CD, CA, YJ, JAR, and LW performed the experiments. CD, CA, ND, NP, MD and LW provided the resources. ED, LJ, YJ and RL performed data curation. ED and LJ analysed the data. ED wrote the original draft. All authors read, revised, and approved the submitted manuscript.

Competing interest statement

The authors declare that there is no conflict of interest.

944 **Figure legends**

945 Figure 1: Bisection of equine embryos at 8 days post-ovulation into an ICMandTE and a TE_part.

946 a) Step 1: Identification of the ICM and the TE; b) Step 2: Definition of the cutting plane to isolate the
947 ICM in one of the parts; c) Step 3: Cutting of the embryo and separation of the two parts. ICMandTE:
948 inner cell mass + trophoblast; TE part: pure trophoblast.

949 NB: Here the trophoblast represents trophectoderm + endoderm and ICM is composed of epiblast
950 cells.

951

952 Figure 2: Effect of embryo size on RNA yield and gene expression in equine embryos

953 a) Green circles represent embryos from young mares (YM) and yellow squares represent embryos
954 from old mares (OM). The used relation is exponential. b) Biplot graphics representing principal
955 component analyses of differentially expressed genes in inner cell mass and trophoblast of embryos
956 collected in YM or OM. Embryo were grouped according to maternal age (YM or OM) and their
957 diameter (< 1100µm = small; > 1100µm = large). The top 20 variables contributing to the axis
958 formation were represented.

959

960 Figure 3: Gene expression in ICM and TE before and after deconvolution using DeMixT

961 A) Venn diagrams of the differential gene expression in ICMandTE *vs* TE part (before deconvolution),
962 DeMixT_ICM_cells *vs* DeMixT_TE_cells (after deconvolution) and DeMixT_ICM_cells *vs* TE_part (gene
963 expression of ICM after deconvolution *vs* gene expression in TE_part without deconvolution); B)
964 Principal Component Analysis of gene expression of DeMixT_ICM_cells, DeMixT_TE_cells, ICMandTE
965 and TE part datasets.

966 Deconvolution was used to isolate gene expression of ICM and TE cells in ICMandTE hemi-embryos.
967 ICMandTE: inner cell mass + trophoblast; TE part: pure trophoblast. Here trophoblast represents
968 trophectoderm + endoderm.

969

970 Figure 4: Analysis of differentially expressed genes (DEG) in embryos according to maternal age

971 A) representation of down (blue) and upregulated (red) DEG in ICM (from DeMixT_ICM_cells data
972 obtained after deconvolution of ICMandTE using DeMixT R package [101,102]) and TE (from TE_part
973 dataset) of embryos from OM *vs* YM. Functional classifications (for down regulated genes in ICM and
974 TE and for up-regulated genes in ICM) using GO Biological Process obtained with PANTHER online
975 software are presented as pie charts. For upregulated DEG in TE, no functional classification was
976 made.

977 B) Bar chart presenting p-adjusted of most specific subclass pathways provided by PANTHER online
978 software after statistical overrepresentation test (Fisher's Exact test and Benjamini-Hochberg
979 correction) with the Human GO Biological Process annotation on down-regulated DEGs in ICM.

980 DEG: Differentially Expressed Genes (FDR < 0.05); TE: Trophoblast; ICM: Inner Cell Mass; OM: Old
981 multiparous mares; YM: young multiparous mares

982

983 Figure 5: GSEA clustering of the most perturbed terms in ICM and TE according to mares' age

984 Nodes represent altered gene sets in ICM and TE (FDR < 0.05). Node size represents the gene set size.
985 Node shape represents the gene set database: GO BP (circle) or KEGG (diamond). Blue nodes
986 represent enriched gene sets in YM (NES < 0) while red nodes represent enriched gene sets in OM
987 (NES > 0). Edges represent the level of connection between representative gene sets. This graph was
988 performed using SUMER R package [114] and modified using cytoscape 3.8.2 [115]

989 ICM: Inner Cell Mass; TE: trophoblast; FDR: False Discovery Rate; GO BP: Gene Ontology Biological
990 Process; Kyoto Encyclopedia of Genes and Genomes; NES: Normalized Enrichment Score; YM: Young
991 mares; OM: Old mares

992

993 Figure 6: Schematic representation of the observed effects of maternal aging on ICM and TE in
994 equine blastocysts

995 Normal blastocyst development from day 7 to day 9 is represented inside black square using
996 literature [47,48]. Light blue boxes represent biological processes that are enriched in YM embryos and
997 light red boxes represent biological processes that are enriched in OM embryos.

998

999

1000 **Tables**

1001 Table 1: Mares' characteristics at embryo collection time.

Characteristics	**Young mares (YM)** ***(n = 11)***		**Old mares (OM)** ***(n=20)***	
	Total	**With embryo (n = 5)**	**Total**	**With embryo (n = 6)**
Breed	AA n = 9; SF n =1; SB n=1	AA	AA n = 13; SF n = 7	AA n = 4; SF n = 2
Age *(in years)*	6.00 ± 0.00	6.00 ± 0.00	11.95 ± 2.11	12.00 ± 2.90
Parity *(number of foalings)*	1.00 ± 0.00	1.00 ± 0.00	3.20 ± 1.15	3.17 ± 1.47
Weight *(in kg)*	536.62 ± 44.12	524.02 ± 61.39	589.35 ± 57.34	598.19 ± 76.83
BCS *(scale 1-5)*	2.16 ± 0.28	2.3 ± 0.33	2.61 ± 0.32	2.5 ± 0.59
Withers' height *(in cm)*	157.95 ± 3.74	157.40 ± 5.41	161.21 ± 4.23	162.00 ± 6.16

1002 All mares were multiparous.

1003 AA: Anglo Arab or Anglo-Arabian type; SF: Selle Français; SB: Saddlebred; BCS: Body Condition Score.

1004 Age, parity, weight, BCS and height are presented as mean ±SD

1005

1006

1007 Table 2: Comparison of selected genes expression before and after deconvolution

	Gene name	Ensembl ID	ICMandTE *vs* TE_part		DeMixT_ICM_cells *vs* TE_part	
			log2FC from DeSeq2	padj	log2FC from DeSeq2	Padj
ICM	**SOX2**	ENSECAG00000010653	4.49	0.02	6.49	1.7E-06
	NANOG	ENSECAG00000012614	4.24	1.0E-07	5.98	2.4E-15
	SPP1	ENSECAG00000017191	4.02	8.4E-09	5.74	5.1E-16
	LIN28B	ENSECAG00000020994	3.23	1.3E-10	5.00	4.7E-22
	SMARCA2	ENSECAG00000024187	0.62	0.97	1.25	0.07
	POU5F1 (OCT4)	ENSECAG00000008967	0.60	0.009	-2.04	4.6E-07
	ID2	ENSECAG00000008738	0.44	0.29	1.24	9.0E-05
	DNMT3B	ENSECAG00000012102	0.35	0.24	0.8	0.06
	DPPA4	ENSECAG00000013271	0.35	0.04	1.14	1.8E-05
	SALL4	ENSECAG00000018533	0.10	1	0.60	0.01
	KLF4	ENSECAG00000010613	-0.04	1	-0.81	0.39
	UTF1	ENSECAG00000039888	-0.13	1	-2.21	7.3E-05
TE	**TFAP2A**	ENSECAG00000017468	-0.17	0.46	-0.30	0.004
	CDX2	ENSECAG00000027754	-0.14	0.77	-0.23	0.07
	ELF3	ENSECAG00000014608	-0.13	1	-0.19	0.27
	GATA2	ENSECAG00000016768	-0.13	1	-0.29	0.048
	GATA3	ENSECAG00000024574	-0.10	0.87	-0.05	0.64
	TEAD4	ENSECAG00000011303	-0.10	0.96	0.00	1
	FREM2	ENSECAG00000020410	0.07	1	0.19	0.44

1008

1009 Gene expressions were obtained from RNA of 11 equine embryos bissected in two hemi-embryos:
1010 one part is composed only of trophoblast (TE), TE_part, while the other part is composed of TE and
1011 inner cell mass (ICM), ICMandTE. As it is impossible to estimate the proportion of each cells in
1012 ICMandTE, deconvolution algorithm (package DeMixT) was used to estimate gene expression of
1013 these different kind of cells. DeMixT_ICM_cells dataset is the deconvoluted gene expression of ICM
1014 cells from ICMandTE. Log2 fold change (log2FC) and padj (adjusted p-value with Benjamini-Hochberg

1015 correction) were obtained with Deseq2 package. TE_part is the reference group in both analyses:
1016 when log2 fold changes (log2FC) > 0, gene is more expressed in ICMandTE or DeMixT_ICM_cells
1017 while when log2FC < 0, gene is more expressed in TE_part. Green is used to represent gene
1018 differentially expressed in the present study. Orange is used to represent gens that have been
1019 previously identified as predominant in the ICM [35] but which are identified here as predominant in
1020 the TE.

1021

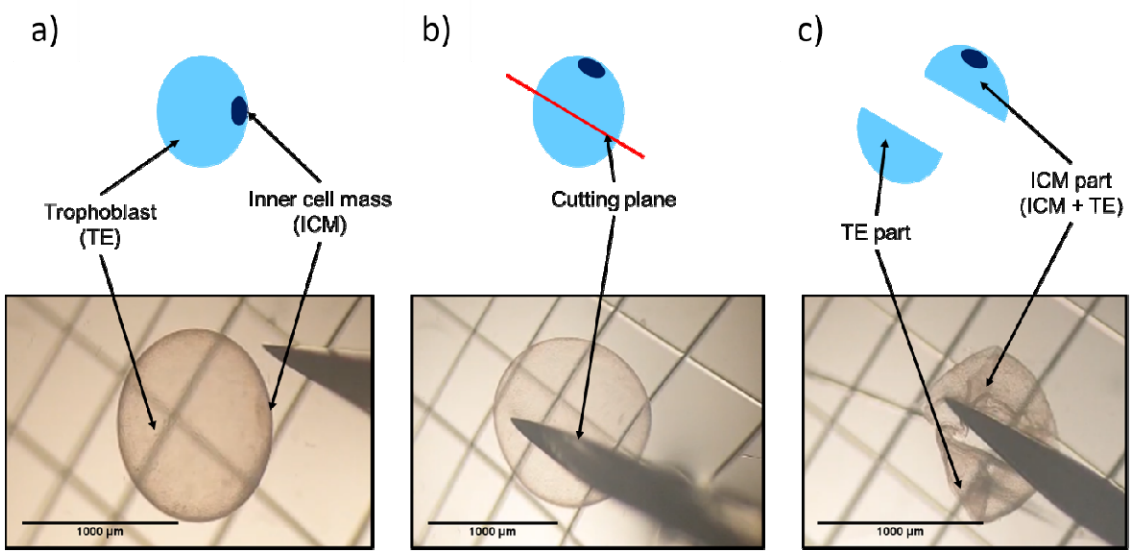
a)
Trophoblast
(TE)
Inner cell mass
(ICM)
1000 µm
b)
Cutting plane
1000 µm
c)
TE part
ICM part
(ICM + TE)
1000 µm

a)

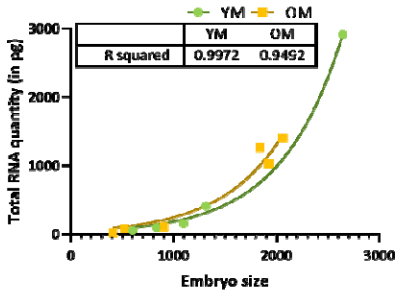
YM
OM
Total RNA quantity (in pg)
Embryo size
R squared
0.9972
0.9492
0
1000
2000
3000

b)

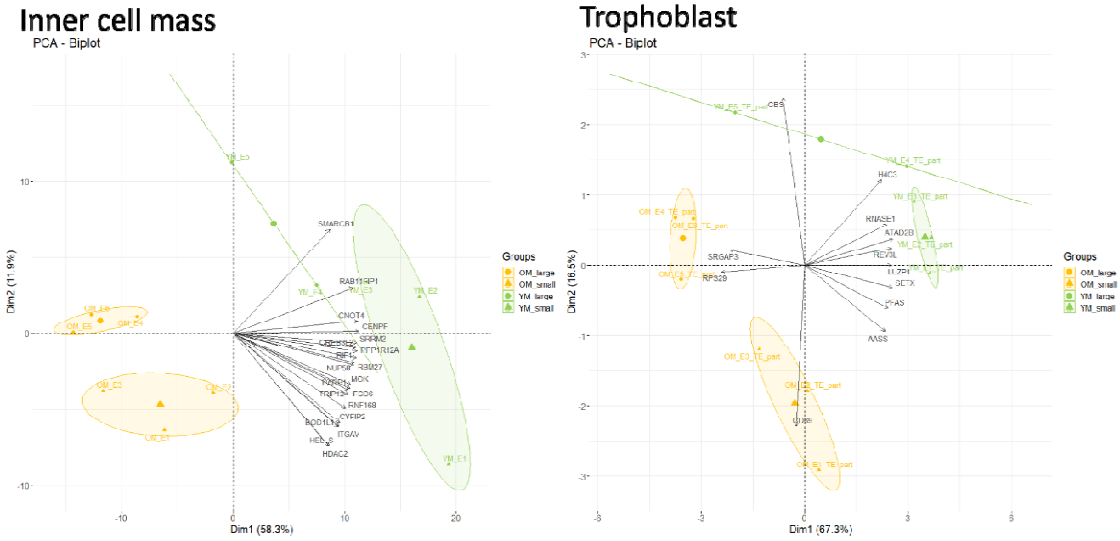
Inner cell mass
PCA - Biplot
Dim1 (58.3%)
Dim2 (11.9%)
Groups
OM_large
OM_small
YM_large
YM_small
Trophoblast
PCA - Biplot
Dim1 (67.3%)
Dim2 (18.5%)
Groups
OM_large
OM_small
YM_large
YM_small

1024

1025

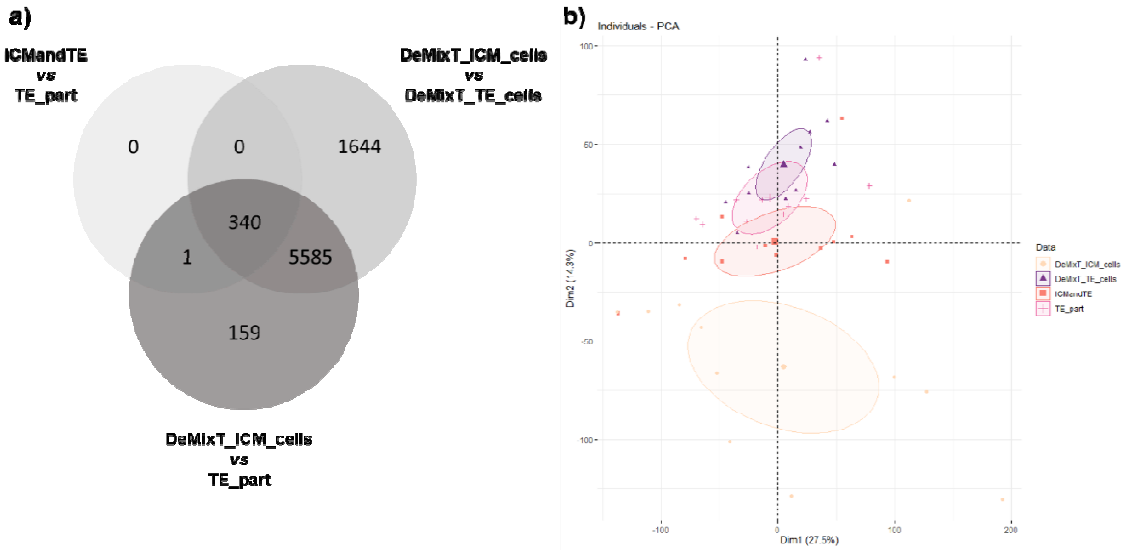
a)
ICMandTE
vs
TE_part
DeMixT_ICM_cells
vs
DeMixT_TE_cells
0
0
1644
340
1
5585
159
DeMixT_ICM_cells
vs
TE_part
b)
Individuals - PCA
Dim1 (27.5%)
Dim2 (14.3%)
Data
DeMixT_ICM_cells
DeMixT_TE_cells
ICMandTE
TE_part

1026

1027

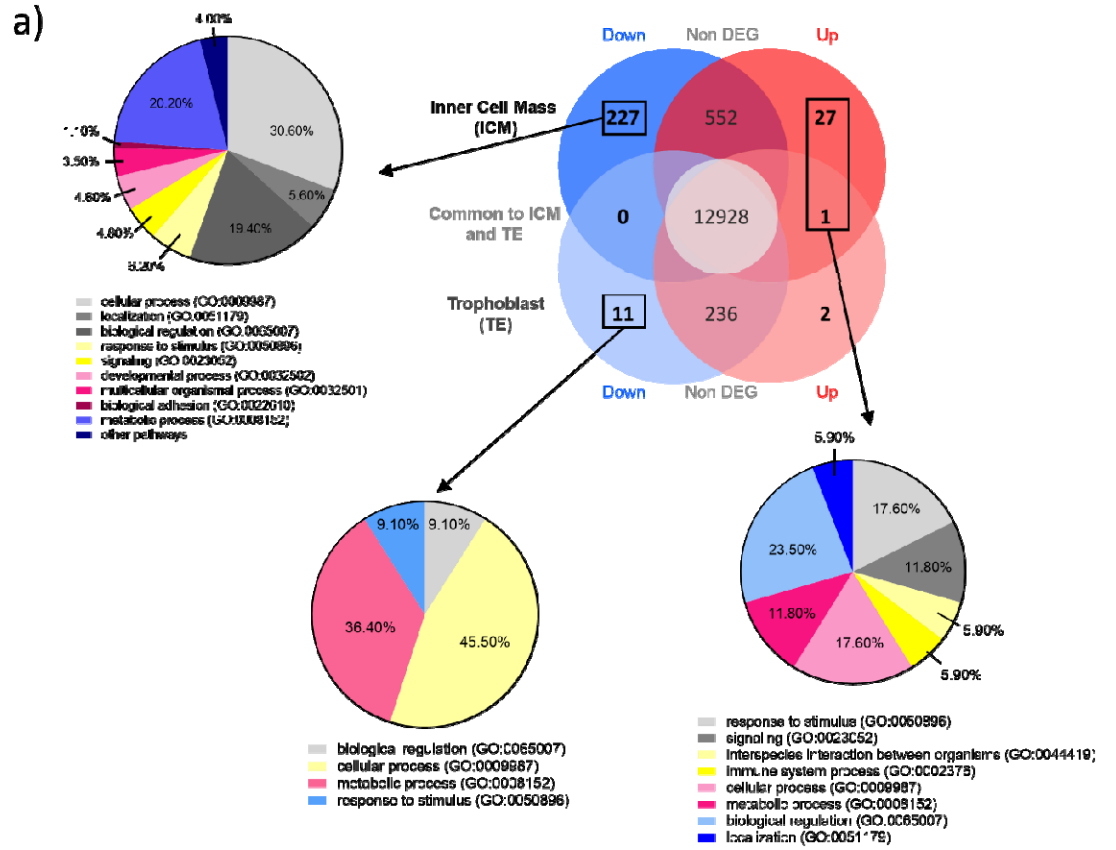
a)
Down
Non DEG
Up
Inner Cell Mass (ICM)
227
552
27
Common to ICM and TE
0
12928
1
Trophoblast (TE)
11
236
2
Down
Non DEG
Up
30.60%
5.60%
19.40%
20.20%
3.50%
4.60%
4.00%
cellular process (GO:0009987)
localization (GO:0051179)
biological regulation (GO:0065007)
response to stimulus (GO:0050896)
signaling (GO:0023052)
developmental process (GO:0032502)
multicellular organismal process (GO:0032501)
biological adhesion (GO:0022610)
metabolic process (GO:0008152)
other pathways
9.10%
9.10%
36.40%
45.50%
biological regulation (GO:0065007)
cellular process (GO:0009987)
metabolic process (GO:0008152)
response to stimulus (GO:0050896)
5.90%
17.60%
11.80%
23.50%
11.80%
17.60%
5.90%
5.90%
response to stimulus (GO:0050896)
signaling (GO:0023052)
interspecies interaction between organisms (GO:0044419)
immune system process (GO:0002376)
cellular process (GO:0009987)
metabolic process (GO:0008152)
biological regulation (GO:0065007)
localization (GO:0051179)

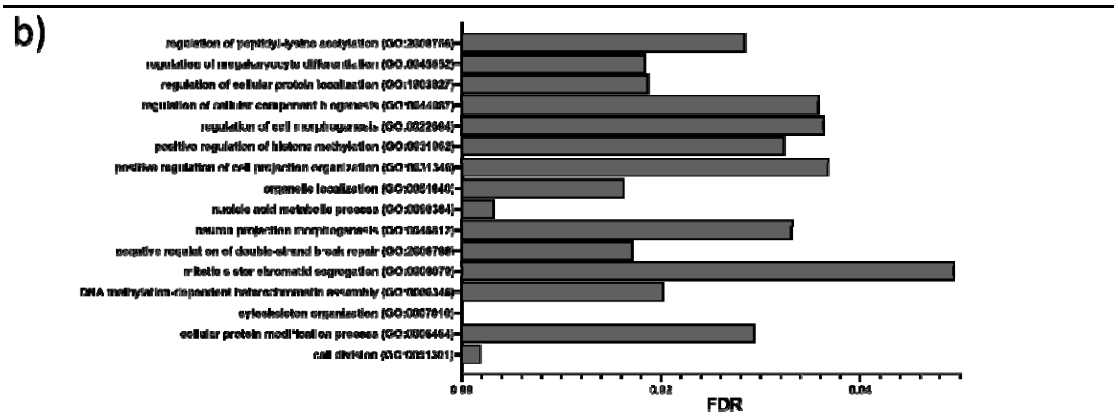
b)
regulation of peptidyl-lysine acetylation (GO:2000756)
regulation of megakaryocyte differentiation (GO:0045652)
regulation of cellular protein localization (GO:1903827)
regulation of cellular component biogenesis (GO:1904437)
regulation of cell morphogenesis (GO:0022604)
positive regulation of histone methylation (GO:0031062)
positive regulation of cell projection organization (GO:0031346)
organelle localization (GO:0051640)
nucleic acid metabolic process (GO:0090304)
neuron projection morphogenesis (GO:0048812)
negative regulation of double-strand break repair (GO:2000785)
mitotic sister chromatid segregation (GO:0000070)
DNA methylation-dependent heterochromatin assembly (GO:0006346)
cytoskeleton organization (GO:0007010)
cellular protein modification process (GO:0006464)
cell division (GO:0051301)
0.00
0.02
0.04
FDR

1028

1029

Inner Cell Mass

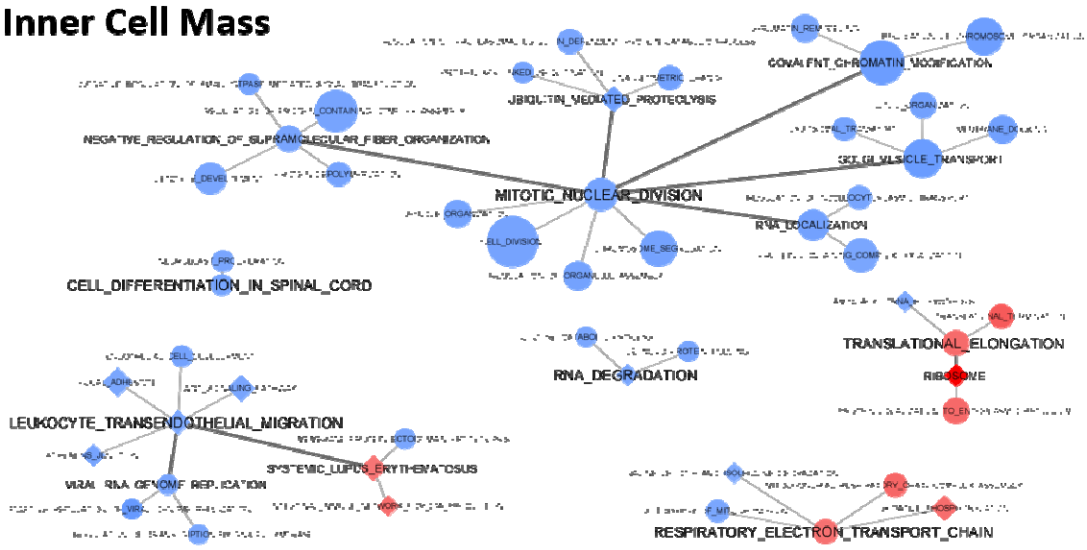

Trophoblast

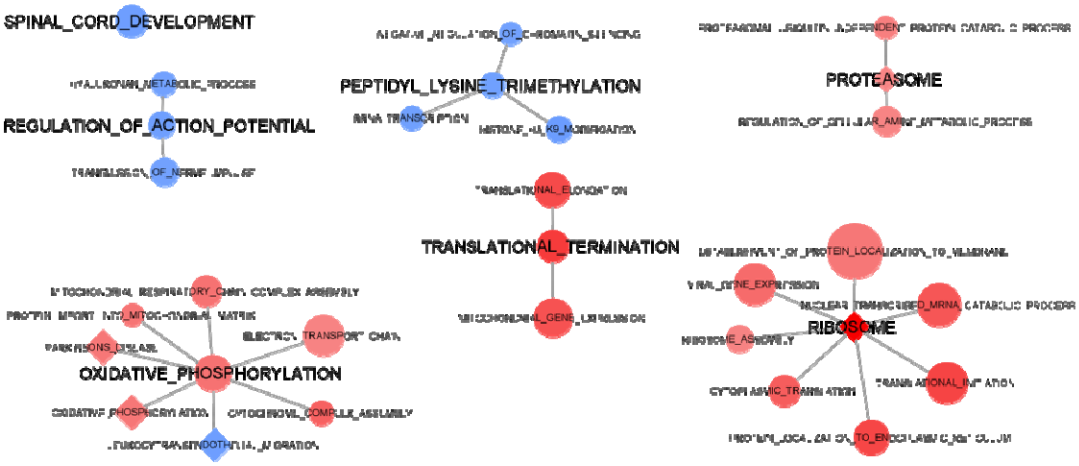

1030

1031

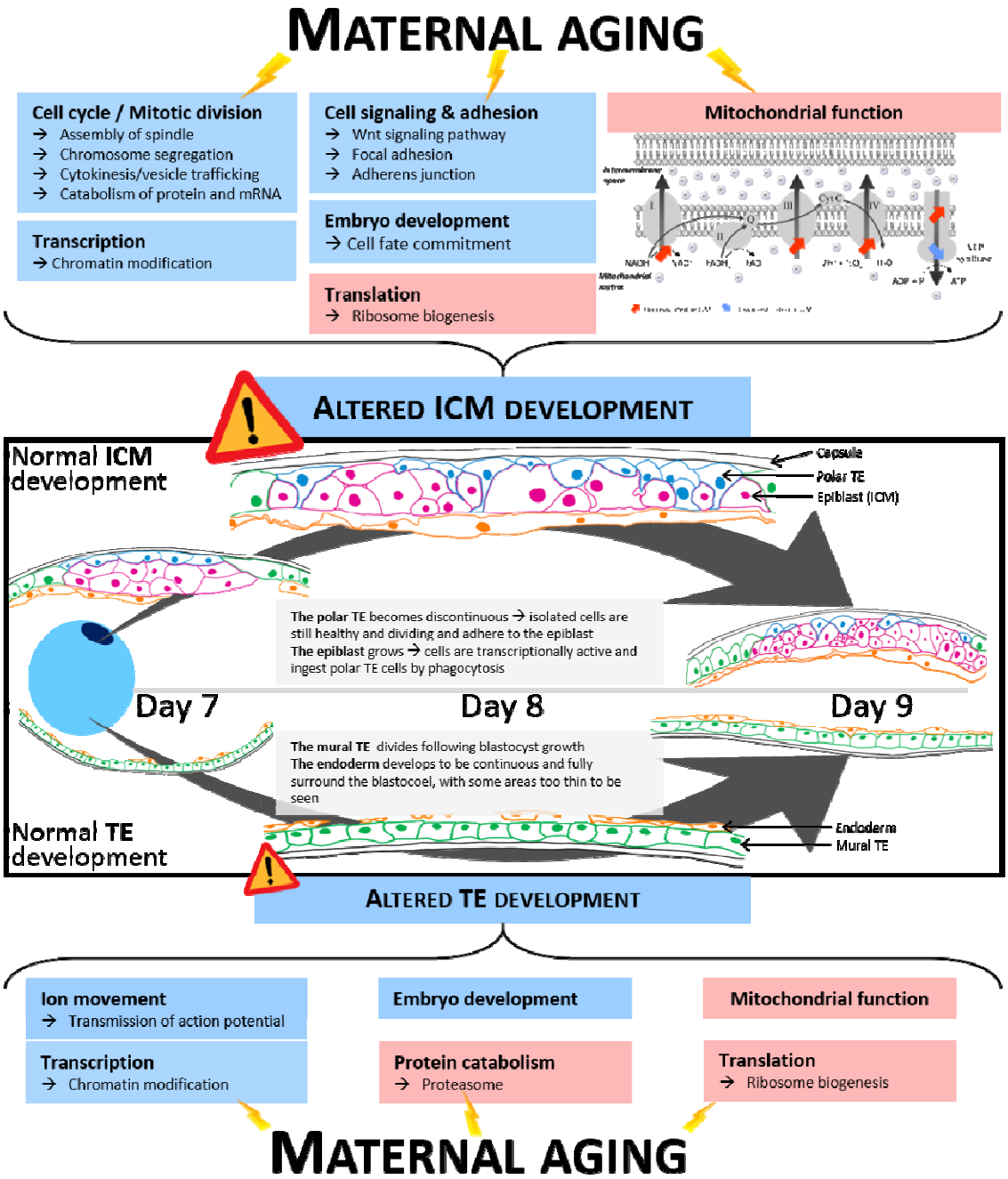
MATERNAL AGING
Cell cycle / Mitotic division
→ Assembly of spindle
→ Chromosome segregation
→ Cytokinesis/vesicle trafficking
→ Catabolism of protein and mRNA
Transcription
→ Chromatin modification
Cell signaling & adhesion
→ Wnt signaling pathway
→ Focal adhesion
→ Adherens junction
Embryo development
→ Cell fate commitment
Translation
→ Ribosome biogenesis
Mitochondrial function
ALTERED ICM DEVELOPMENT
Normal ICM development
Capsule
Polar TE
Epiblast (ICM)
The polar TE becomes discontinuous → isolated cells are still healthy and dividing and adhere to the epiblast
The epiblast grows → cells are transcriptionally active and ingest polar TE cells by phagocytosis
Day 7
Day 8
Day 9
The mural TE divides following blastocyst growth
The endoderm develops to be continuous and fully surround the blastocoel, with some areas too thin to be seen
Normal TE development
Endoderm
Mural TE
ALTERED TE DEVELOPMENT
Ion movement
→ Transmission of action potential
Transcription
→ Chromatin modification
Embryo development
Protein catabolism
→ Proteasome
Mitochondrial function
Translation
→ Ribosome biogenesis
MATERNAL AGING

1032

1033